CONOTOXINS: DISCOVERY USING NEW ASSAYS AND APPLICATIONS IN THE CHARACTERIZATION OF PRURICEPTORS IN THE MOUSE DORSAL ROOT GANGLION (DRG)

by

Samuel Sindingan Espino

A dissertation submitted to the faculty of
The University of Utah
in partial fulfillment of the requirements for the degree of

Doctor of Philosophy

Department of Biology

The University of Utah

December 2016

The University of Utah Graduate School

STATEMENT OF DISSERTATION APPROVAL

The dissertation of **Samuel Sindingan Espino**

has been approved by the following supervisory committee members:

Baldomero M. Olivera	, Chair	**Sept. 28, 2016** Date Approved
David F. Blair	, Member	**Sept. 28, 2016** Date Approved
Grzegorz Bulaj	, Member	**Sept. 28, 2016** Date Approved
Eric Jorgensen	, Member	**Sept. 28, 2016** Date Approved
Andres Villu Maricq	, Member	**Sept. 28, 2016** Date Approved

and by **Denise Dearing** , Chair/Dean of

Department/College/School of **Biology**

and by David B. Kieda, Dean of The Graduate School.

ABSTRACT

Cone snails are predatory marine gastropods that use venom to capture prey. Components of the cone snail venom are small peptidic compounds called conotoxins which target ion channels, receptors, and transporters in the prey's nervous system. Conotoxins are highly potent and specific towards their molecular target, thus, they are used as tools for the understanding of how the nervous system works. Moreover, conotoxins are also powerful leads for developing new drugs. A conotoxin, ω-MVIIA is now sold as the drug Prialt for the treatment of pain.

Given the tremendous research and pharmacological applications of these compounds, it is thus important to pursue further research aimed at discovering novel conotoxins. For this research I aimed to discover novel conotoxins using two biological assays that were not previously used in conotoxin discovery. One assay measured the activity of the norepinephrine transporter (NET) expressed in human embryonic kidney (HEK) cells to reuptake radiolabeled norepinephrine and another assay used calcium imaging of dissociated mouse dorsal root ganglion (DRG) neurons. Further, I focused my research on cone snail clades with limited toxinological information.

Chapter 2 describes two conotoxins whose activities were identified using the NET assay. These conotoxins χ-AuID and χ-AoIC were isolated from the

venom of mollusk-hunters *Conus aulicus* and *Conus araneosus,* respectively. The conotoxin fv1a from *Conus furvus* another mollusk-hunting cone snail is also reported. The conotoxin fv1a does not inhibit NET, however, this conotoxin shows activity *in vivo* in mice and in calcium imaging of DRG neurons. The three conotoxins presented in Chapter 2 are homologous, however, they do not have the same pharmacological property. Thus, a comparison of the sequences of χ-AuID, χ-AoIC, and fv1a allowed for the identification of amino acids important for NET inhibition.

Chapter 3 describes glycine-rich conotoxins identified from the venom of worm-hunting snails in the *Virgiconus* clade. vi6a, the first conotoxin identified in this group, was purified from the venom of *Conus virgo* using calcium imaging. This conotoxin elicited an excitatory behavior in mice when injected intracranially (IC) and intraperitoneally (IP). Conotoxins homologous to vi6a were further identified from *Conus terebra* and *Conus kintoki* using molecular biology techniques. Interestingly, *C. virgo* expresses two additional conotoxins homologous to vi6a.

Chapter 4 describes the characterization of pruriceptors in the mouse DRG that are responsive to histamine and chloroquine. Three major populations of neurons were identified and these populations were further characterized using various pharmacological agents to identify the constellation of ion channels and receptors expressed in the membrane of these neurons. Using the conotoxin μ-PIIIA, the expression of Nav1.7 and Nav1.8 in these pruriceptor populations were identified.

TABLE OF CONTENTS

ABSTRACT iii

LIST OF TABLES vii

LIST OF FIGURES viii

Chapters

1. INTRODUCTION 1

    Dissertation outline 7
    References 11

2. T-SUPERFAMILY CONOTOXINS FROM MOLLUSK-HUNTING CONE SNAILS: BIOLOGICAL ACTIVITY AND INHIBITION OF THE NOREPINEPHRINE TRANSPORTER (NET) 17

    Abstract 18
    Introduction 18
    Materials and methods 21
    Results 28
    Discussion 33
    References 53

3. GLYCINE-RICH CONOTOXINS FROM THE VIRGICONUS CLADE 57

    Abstract 58
    Introduction 58
    Materials and methods 59
    Results 60
    Discussion 62
    References 64

4. FUNCTIONAL CHARACTERIZATION OF PRURICEPTORS IN THE MOUSE DORSAL ROOT GANGLION (DRG) 65

    Abstract 66

Introduction 66
Materials and methods 69
Results 71
Discussion 75
References 87

5. SUMMARY 91

Pharmacologically distinct peptides in the T-superfamily 92
Glycine-rich conotoxins in the O1-superfamily 94
Pruritogen-sensitive neurons in the mouse dorsal root ganglion (DRG)… 96
Future research 98
References 103

LIST OF TABLES

1.1 Conotoxins undergoing various stages of clinical trial……10

2.1 T-superfamily conotoxins presented and discussed in this paper…….52

3.1 Biological activity of vi6a injected IC and IP into 17-19 day old mice…...64

4.1 Challenge compounds used in experiments conducted in this research……..…86

5.1 Conotoxins in the O1-superfamily……102

LIST OF FIGURES

2.1 Phylogenetic relationships in mollusk-hunting cone snails……..…38

2.2 Purification of χ-AuID……...40

2.3 Purification of fv1a…….42

2.4 Co-elution experiment of native and synthetic c-AuID and fv1a……44

2.5 Activity of χ-AuID, χ-AoIC, and fv1a against human norepinephrine transporter (hNET) expressed in HEK-293 cells……...…46

2.6 Sequence alignment of the precursors of fv1a, χ-AuID, and χ-MrIA…….48

2.7 Comparison of the effects of fv1a and the χ-conotoxins on the response of DRG neurons to depolarization by 25 mM KCl…….…..50

3.1 Phylogenetic relationships in the *Virgiconus* clade…….…..59

3.2 Bioactivity-guided purification of the inhibitory component from *C. virgo* venom……..……61

3.3 Alignment of conotoxin sequences predicted from clones obtained from *C. virgo* (Vi), *C. terebra* (Tr), and *C. kintoki* (Kt)……...…62

3.4 Alignment of the precursor sequence of vi6a (Vi6.1) with the Precursor sequence of conotoxins identified from *C. virgo*, *C. terebra,* and *C. kintoki*…….……..……63

4.1 Responses of DRG neurons to the application of histamine and chloroquine and other challenge compounds……...81

4.2 Voltage-gated sodium channel (VGSC) expression in the class A (His+) cells, class B (Caps+) cells and in class C (CQ+, AITC+) cells.....84

5.1 Sequence alignment of T-superfamily conotoxins from mollusk-hunting cone snails…….…100

CHAPTER 1

INTRODUCTION

Cone snails (genus *Conus*) comprise a large group of predatory marine gastropods that inhabit the tropical waters around the world. This genus is species rich with ~850 known members and all of them use venom for various biotic interactions, including prey capture (Favreau and Stocklin 2009; Olivera 2002; Röckel et al. 1995). There are three major groups of cone snails based on prey, these are fish-hunting (piscivores), mollusc-hunting (molluscivores) and the largest group, worm-hunting (vermivores) (Kohn 1959; McIntosh and Jones 2001; Olivera 1997; Olivera et al. 1990).

Humans have shown interest in cone snails since the dawn of civilization. An excavation form the ancient Mesopotamian city of Uruk discovered a 5000 year old necklace made of cone snail shells (Terlau and Olivera 2004; Olivera et al. 2014). The keen interest of humans in cone snails is not surprising since cone snails possess arguably some of the most beautiful shells known to man. For example, a rare specimen of *Conus cedonulli* (the matchless cone) was priced higher than the painting “Woman in Blue Reading a Letter” by the Dutch master Johannes Vermeer at an auction in Europe in the late 18th century (Terlau and Olivera 2004; Olivera et al. 2014).

In some islands in the central Philippines, the cone snails, although not very abundant, are a food source for the local population. These snails can even be purchased in the local market. The snails are usually cooked with noodles or prepared as a broth flavored with local spices. The locals report that the best tasting part of the snail is the foot whereas other parts of the cone snail have a gritty texture.

The scientific interest in cone snails stems from the fact that cone snail stings are extremely painful and some human stinging incidents proved fatal. One species for example, *Conus geographus* (the geography cone) has caused multiple human fatalities (Flecker 1936; Fegan and Andresen 1997). Other cone snail species are not as deadly as *C. geographus,* however, they can still deliver painful stings. People living in coastal areas in the Philippines know to be extra careful when handling all species of cone snails.

Cone snails deliver lethal or painful stings because of the venom that the snail injects. Venom is made in the snail's venom gland. Attached to this gland is a muscular bulb that functions to push the venom out of the gland into the proboscis. At the tip of the proboscis is a radular tooth that pierces the prey and delivers venom (Olivera 2002). In some species, the tip of the radular tooth is barbed such that when the prey is stung it is effectively tethered to the snail (Kantor and Puillandre 2012; Olivera 1997). The components of the venom are called conotoxins/conopeptides which target ion channels, receptors, and transporters in the nervous system of the prey animals, predators, or competitors (Lebbe et al. 2014; Adams et al. 2012; Schroeder and Craik 2012). The conotoxins are small peptidic molecules generally 10 – 30 amino acids long (Olivera et al. 1985; Gray et al. 1988). The small size of these conotoxins is unique since peptidic venom components from other species are relatively large comprising of 40 – 80 amino acids (Olivera et al. 1990). Another striking feature of conotoxins is the abundance of posttranslationally modified amino acids. These modifications include the hydroxylation of proline (Cruz et al. 1985; Lopez-

Vera et al. 2008), the glycosylation of threonine and serine (Craig et al. 1998; Craig et al. 1999), bromination of tryptophan (Rigby et al. 1999; Jimenez et al. 2004), γ-carboxylation of glutamate (Bandyopadhyay et al. 1998; Rivier et al, 1987), sulfation of tyrosine (Wolfender et al. 1999), and conversion of L- to D-amino acids (Buczek et al. 2005a; Buczek et al. 2008). Conotoxins are translated through conventional ribosomal pathways and the mRNA's coding for each of these conotoxins can be isolated from the venom duct.

Conotoxins are translated as a precursor with three distinct regions (Buczek et al. 2005b; Olivera 1997). The canonical conotoxin precursor consists of the signal sequence at the N-terminal, an intervening proregion, and the toxin coding region located at the C-terminal (Colledge et al. 1992; Robinson and Norton 2014). Analysis of the conotoxin precursor identified from different cone snail species revealed that conotoxins with conserved pattern of cysteine residues in the mature toxin have a correspondingly highly conserved sequence of amino acids in the signal sequence (Woodward et al. 1990; Santos et al. 2004; Corpuz et al. 2005; Walker et al. 1999). The conotoxins that display this pattern of conservation of amino acids in their precursor belong to the same gene superfamily (Terlau and Olivera 2004; Woodward et al. 1990). Moreover, conotoxins under a gene superfamily with the same pharmacological target fall under a conotoxin family (Terlau and Olivera 2004). For example, conotoxin family in the O1-superfamily include the ω-conotoxins, which target voltage-gated calcium channels (Hillyard et al. 1992; Olivera et al. 1985; Zhangsun et al. 2006), the κ-conotoxins, which target voltage-gated potassium channels (Shon et al.

1998; Terlau et al. 1996), and the δ- and the μO-conotoxin families, which target different sites in voltage-gated sodium channels (Leipold et al. 2005; McIntosh et al. 1995; Shon et al. 1995; Terlau et al. 1996; Wilson et al. 2015).

Conotoxins are evolved to be fast acting and extremely potent towards their ion channel and receptor target. This is expected since cone snails are slow moving animals that lack mechanical features that can be used to their advantage for predation, warding off competitors, or for defense. The molecular diversity of potential ion channel or receptor targets provides the evolutionary stimulus for the cone snails to develop a complex complement of fast acting peptides in their venom (Olivera and Teichert 2007).

Homologues of ion channels and receptors in the snails prey, predator or competitor are also expressed by mammals. For example, injection of specific componen purified from the venom of the fish-hunting *C. geographus* into mice elicited aberrant behavior which include hyperactivity, shaking, scratching, excessive grooming, sleeping, sluggishness, seizures, barrel rolling, and, in some cases, death (Olivera et al. 1990). Research has shown that conotoxins has the ability to discriminate molecular isoforms of a particular ion channel family (Favreau et al. 1999; Olivera and Teichert 2007). Many of these ion channels exist in heteromeric combinations thus the number of possible isoforms of these ion channels is immensely large. For example, the voltage-gated potassium channel can be assembled from more than 80 gene products to create the functional tetrameric channel (Hille 2001; Jan and Jan 1997). The ability to discriminate related isoforms of a particular ion channel or receptor is especially

important for defining the physiological function of a specific ion channel isoform.

An important implication that resulted from these studies is that conotoxins can be used to modulate the activity of their molecular targets. What this means is that conotoxins can be used as drugs for pathologies where their molecular target is involved. One conotoxin, ω-MVIIA, from *Conus magus* is in the market as Ziconotide (Prialt) used for the treatment of severe chronic pain (Klotz 2006; Sanford 2013; Williams et al. 2008). Several other conotoxins are undergoing different stages of clinical trials for the treatment of various diseases (Table 1.1).

Conotoxins are also used to probe the cell surface expression of their specific target. In a method called constellation pharmacology, conotoxins have proved useful in identifying cell surface expression of ion channels and receptors in populations of neurons and glia in the mouse nervous system. Constellation pharmacology uses calcium imaging to monitor cytosolic fluxes of calcium in a population of neuronal cells exposed to multiple compounds including conotoxins (Teichert et al. 2012; Smith et al. 2013). A change in cytosolic calcium in response to any of these compounds indicates the cell surface expression of the receptor for that compound. For example, an increase in cytosolic calcium in response to the application of capsaicin indicates the presence of TrpV1 the capsaicin receptor. A series of application of these compounds identifies a group or a constellation of ion channels and receptor present in each of the cells in the experiment. Cells with the same profile of ion channels and receptor expression belong to a specific cell type. The identification of these cell types and the corresponding ion channels and receptors expressed by these cell types is an

important step in defining the physiological function mediated by these cells. Moreover, knowing the ion channels and receptors in these cell types also identifies potential pharmacological targets in conditions where a cell type is involved in particular disease.

Of the ~850 species of cone snail, only a small fraction of this number has been thoroughly probed for the conotoxins they express. Toxinological studies of cone snail involve testing the venom for activity against mice, a vertebrate animal. Thus, most of the cone snail species whose venom has been thoroughly researched belong to a group that hunts vertebrates: the fish-hunting cone snails. However, the mollusk- and the worm-hunting cone snails also express venom components that are active against ion channels or receptors expressed by vertebrates. The worm-hunting cone snails comprise the largest cone snail group, thus, there is still a huge number of cone snail species with very limited information about their venom. The characterization of conotoxins from these less studied cone snail species is important because these conotoxins have the potential to have unique biological and pharmacological activities and will prove extremely useful in research and drug development.

Dissertation outline

For my dissertation, I made an attempt to purify and characterize conotoxins from mollusk- and worm-hunting snails. The cone snail species chosen for this work belong to clades where toxinological data are very limited. To achieve my goal, I will use bioactivity guided purification to purify the

conotoxins from venom and biochemically deduce the toxin sequence. Two kinds of assays were used in this research. One assay used calcium imaging to screen the venom for activity against a culture of mouse dorsal root ganglion (DRG) neurons, and another assay screened the venom for activity against a known molecular target, the norepinephrine transporter (NET). One of the major motivations in conducting this research is the fact the conotoxins are powerful tools in studying the nervous system. To illustrate, I used the conotoxin μ-PIIIA one of the pharmacological agents utilized to identify the expression of ion channels and receptors in a subset of DRG neurons that are sensitive to pruritogens. Chapter 2 of my dissertation describes a family of conotoxins identified from the *Virgiconus* clade. Members of this clade hunt worms. The first conotoxin in this family was purified from the venom of *Conus virgo* by following its ability in calcium imaging experiments to partially inhibit the increase in cytosolic calcium upon depolarization by external application of potassium chloride (KCl). These conotoxins are unusually glycine-rich and are expressed by members of the clade across a wide range of habitat. Chapter 3 talks about conotoxins from mollusk-hunting cone snails that belong to the T-superfamily. Three conotoxins are described in this chapter. Two conotoxins inhibit the reuptake of norepinephrine through the norepinephrine transporter (NET). Another conotoxin, although related to the NET-inhibiting conotoxins, does not inhibit NET at the concentrations used in the research. This conotoxin, however, is biologically active upon intra-cranial (IC) injection into young mice (17 – 21 days old) and in the calcium imaging of dissociated mouse dorsal root ganglion

(DRG) neurons. In Chapter 4, I characterized populations of DRG neurons that respond to pruritogens. The characterization of these neurons involved using several pharmacological agents including conotoxins to probe for plasma membrane expression of ion channels and receptors in these populations of pruritogen-sensitive DRG neurons. In Chapter 5, I will summarize the results and look at the big-picture implications of my research. I will also discuss potential researches that can be done based on the data I gathered in the conduct of my dissertation.

Table 1.1: Conotoxins undergoing various stages of clinical trial.

Conotoxin	Cone snail species	Prey	Clinical application	Target	Clinical status	References
ω-MVIIA (Ziconotide, Prialt)	*C. magus*	fish	Pain	Cav2.2	FDA approved	Miljanich 2004
ω-CVID (AM336)	*C. catus*	fish	Pain	Cav2.2	Phase I	Scott et al. 2002
Contulakin-G (CGX-1160)	*C. geographus*	fish	Pain	Neurotensin receptor	Phase I	Craig et al. 1999
α-Vc1.1 (ACV1)	*C. victoriae*	mollusk	Pain	nAChR	Phase II	Satkunanthan et al. 2005
χ-Mrla (XEN2174)	*C. marmoreus*	mollusk	Pain	Norepinephrine transporter	Phase II	Nielsen et al. 2005
Conantokin G (CGX-1007)	*C. geographus*	fish	epilepsy	NMDA receptor	Phase I	Barton and White 2004
κ-PVIIA (CGX-1051)	*C. purpurascens*	fish	Myocardial infarction	Kv1	Preclinical	Lubbers et al. 2005
μO-MrVIB (CGX-1002)	*C. marmoreus*	mollusk	Pain	VGSC	Preclinical	Green et al. 2014

References

Adams D, Callaghan B, Berecki G. 2012. Analgesic conotoxins: block and G protein coupled receptor modulation of N-type (Ca(V)2.2) calcium channels. Br J Pharmacol. 166(2): 486-500.

Bandyopadhyay P, Colledge CJ, Walker CS, Zhou LM, Hillyard D, Olivera BM. 1998. Conantokin-G precursor and its role in gamma-carboxylation by a vitamin K-dependent carboxylase from a Conus snail. J Biol Chem. 273(10): 5447- 5450.

Barton ME, White HS. 2004. The effect of CGX-1007 and Cl-1041, novel NMDA receptor antagonists, on kindling acquisition and expression. Epilepsy Res. 59(1): 1-12.

Buczek O, Jimenez EC, Yoshikami D, Imperial JS, Watkins M, Morrison A, Olivera BM. 2008. I(1)-superfamily conotoxins and prediction of single D-amino acid occurrence. Toxicon 51(2): 218-229.

Buczek O[(a)], Yoshikami D, Watkins M, Bulaj G, Jimenez EC, Olivera BM. 2005. Characterization of D-amino-acid-containing excitatory conotoxins and redefinition of the I-conotoxin superfamily. FEBS J. 272(16): 4178-4188.

Buczek O[(b)], Bulaj G, Olivera BM. 2005. Conotoxins and the posttranslational modification of secreted gene products. Cell Mol Life Sci. 62(24): 3067-3079.

Colledge CJ, Hunsperger JP, Imperial JS, Hillyard DR. 1992. Precursor structure of ω-conotoxin GVIA determined from a cDNA clone. Toxicon 30(9): 1111-1116.

Corpuz G, Jacobsen R, Jimenez E, Watkins M, Walker C, Colledge C, Garrett J, McDougal O, Li W, Gray W, Hillyard D, Rivier J, McIntosh JM, Cruz L, Olivera B. 2005. Definition of the M-conotoxin superfamily: characterization of novel peptides from molluscivorous *Conus* venom. J Biol Chem. 44(22): 8176-8186.

Craig AG, Norberg T, Griffin D, Hoeger C, Akhtar M, Schmidt K, Low W, Dykert J, Richelson E, Navarro V, Mazella J, Watkins M, Hillyard D, Imperial J, Cruz LJ, Olivera BM. 1999. Contulakin-G, an O-glycosylated invertebrate neurotensin. J Biol Chem. 274(20): 13752-13759.

Craig AG, Zafaralla G, Cruz LJ, Santos AD, Hillyard D, Dykert J, Rivier JE, Gray WR, Imperial J, Dela Cruz RG, Sporning A, Terlau H, West P, Yoshikami D, Olivera BM. 1998. An O-glycosylated neuroexcitatory conus peptide. Biochemistry 37(46): 16019-16025.

Cruz LJ, Gray WR, Olivera BM, Zeikus R, Kerr L, Yoshikami D, Moczydlowski E.

1985. *Conus geographus* toxins that discriminate between neuronal and muscle sodium channel. J Biol Chem. 260(16): 9280-9288.

Favreau P, Le Gal F, Benoit E, Molgo J. 1999. A review on conotoxins targeting ion channels and acetylcholine receptors of the vertebrate neuromuscular junction. Acta Physiol Pharmacol Ther Latinoam. 49(4): 257-267.

Favreau P, Stocklin R. 2009. Marine snail venom: use and trends in receptor and channel pharmacology. Curr Opin Pharmacol. 9(5): 594-601.

Fegan D, Andresen D. 1997. *Conus geographus* envenomation. The Lancet 349(9066): 1672.

Flecker H. 1936. Cone shell mollusk poisoning with a report of a fatal case. Med J Aust. 1: 464-466.

Gray WR, Olivera BM, Cruz LJ. 1988. Peptide toxins from venomous Cone snails. Annu Rev Biochem. 57: 665-700.

Green BR, Bulaj G, Norton RS. 2014. Structure and function of μ-conotoxins, peptide-based sodium channel blockers with analgesic activity. Future Med Chem. 6(15): 1677-1698.

Hille B. 2001. Ion channels of excitable membrane (3rd ed.). Sunderland MA: Sinauer 814p.

Hillyard DR, Monje VD, Mintz IM, Bean BP, Nadasdi L, Ramachandran J, Miljanich G, Azimi-Zoonooz A, McIntosh JM, Cruz LJ, Imperial JS, Olivera BM. 1992. A new *Conus* peptide ligand for mammalian presynaptic Ca^{2+} channels. Neuron 9(1): 69-77.

Jan LY, Jan YN. 1997. Clone potassium channels from eukaryotes and prokaryotes. Annu Rev Neurosci. 20: 91-123.

Jimenez EC, Watkins M, Olivera BM. 2004. Multiple 6-bromotryptophan residues in a sleep-inducing peptide. Biochemistry 43(38): 12343-12348.

Kantor Y, Puillandre N. 2012. Evolution of the radular apparatus in Conoidea (Gastropoda: Neogastropoda) as inferred from a molecular phylogeny. Malacologia 55(1): 55-90.

Klotz U. 2006. Ziconotide-a novel neuron-specific calcium channel blocker for the intrathecal treatment of severe chronic pain-a short review. Int J Pharmacol Ther. 44(10): 478-483.

Kohn AJ. 1959. The Ecology of *Conus* in Hawaii. Ecol Monograph 29(1): 47-90.

Lebbe E, Peigneur S, Wijesekara I, Tytgat J. 2014. Conotoxins targeting nicotinic acetylcholine receptors: an overview. Mar Drugs 12(5): 2970-3004.

Leipold E, Hansel A, Olivera BM, Terlau H, Heinemann SH. 2005. Molecular interaction of delta-conotoxins with voltage-gated sodium channels. FEBS Lett. 579(18): 3881-3884.

Lopez-Vera E, Waleska A, Skalicky JJ, Olivera BM, Bulaj G. 2008. Role of hydroxyprolines in the in vitro oxidative folding and biological activity of conotoxins. Biochemistry 47(6): 1741-1751.

Lubbers NL, Campbell TJ, Polakowski JS, Bulaj G, Layer RT, Moore J, Gross GJ, Cox BF. 2005. Postischemic administration of CGX-1051, a peptide from cone snail venom, reduces infarct size in both rat and dog models of myocardial ischemia and reperfusion. J Cardiovasc Pharmacol. 46(2): 141-146.

McIntosh JM, Hasson A, Spira ME, Gray WR, Li W, Marsh M, Hillyard DR, Olivera BM. 1995. A new family of conotoxins that blocks voltage-gated sodium channels. J Biol Chem. 270(28): 16796-16802.

McIntosh JM, Jones RM. 2001. Cone venom--from accidental stings to deliberate injection. Toxicon 39(10): 1447-1451.

Miljanich GP. 2004. Ziconotide: neuronal calcium channel blocker for treating severe chronic pain. Curr Med Chem. 11(23): 3029-3040.

Nielsen CK, Lewis RJ, Alewood D, Drinkwater R, Palant E, Patterson M, Yaksh TL, McCumber D, Smith MT. 2005. Anti-allodynic efficacy of the chi-conopeptide, Xen2174, in rats with neuropathic pain. Pain 118(1-2): 112-124.

Olivera B. 2002. Conus venom peptides: reflection from the biology of clades and species. Annu Rev Ecol Syst. 33: 25-47.

Olivera B, Grey WR, Zeikus R, McIntosh JM, Varga J, Rivier J, de Santos V, Cruz LJ. 1985. Peptide neurotoxins from fish-hunting snail. Science 230(4732): 1338-1343.

Olivera B, Showers Corneli P, Watkins M, Fedosov A. 2014. Biodiversity of cone snails and other venomous marine gastropods: evolutionary success through neuropharmacology. Annu Rev Anim Biosci. 2: 487-513.

Olivera B, Teichert R. 2007. Diversity of the neurotoxic Conus peptides: a model for concerted pharmacological discovery. Mol Interv. 7(5): 251-260.

Olivera BM, Rivier J, Clark C, Ramilo C, Corpuz G, Abogadie F, Mena E, Woodward S, Hillyard D, Cruz LJ. 1990. Diversity of Conus neuropeptides. Science 249(4966): 257-263.

Olivera BM. 1997. E.E. Just Lecture, 1996. Conus venom peptides, receptor and ion channel targets, and drug design: 50 million years of neuropharmacology. Mol Biol Cell 8(11): 2101-2109.

Rigby AC, Lucas-Meunier E, Kalume DE, Czerwiek E, Hambe B, Dahlqvist I, Fossier P, Baux G, Roepstorff P, Baleja JD, Furie BC, Furie B, Stenflo J. 1999. A conotoxin from Conus textile with unusual posttranslational modifications reduces presynaptic Ca^{2+} influx. Proc Natl Acad Sci. 96(10): 5758-5763.

Rivier JE, Galyean R, Simon L, Cruz LJ, Olivera BM, Gray WR. 1987. Total synthesis and further characterization of the gamma-carboxyglutamate-containing "sleeper" peptide from *Conus geographus* venom. Biochemistry 26(26): 8508-8512.

Robinson SD, Norton RS. 2014. Conotoxin Gene Superfamilies. Mar Drugs 12(12): 6058-6101.

Röckel D, Korn W, Kohn AJ. 1995. Manual of the Living Conidae. Hemmen, Wiesbaden, Germany: Verlag Christa 517p.

Sanford M. 2013. Intrathecal ziconotide: a review of its use in patients with chronic pain refractory to other systemic or intrathecal analgesics. CNS Drugs 27(11): 989-1002.

Santos AD, McIntosh JM, Hillyard D, Cruz LJ, Olivera BM. 2004. The A-superfamily of conotoxins structural and functional divergence. J Biol Chem. 279(17): 17596-17606.

Satkunanthan N, Livett B, Gayler K, Sandall D, Down J, Khalil Z. 2005. Alpha-conotoxin Vc1.1 alleviates neuropathic pain and accelerates functional recovery of injured neurons. Brain Res. 1059(2): 149-158.

Schroeder C, Craik D. 2012. Therapeutic potential of conopeptides. Future Med Chem. 4(10): 1243-1255.

Scott DA, Wright CE, Angus JA. 2002. Actions of intrathecal conotoxins CVID, GVIA, MVIIA and morphine in acute and neuropathic pain in the rat. Eur J Pharmacol. 451(3): 279-286.

Shon K, Grilley MM, Marsh M, Yoshikami D, Hall AR, Kurz B, Gray WR, Imperial JS, Hillyard DR, Olivera BM. 1995. Purification, characterization and cloning of the lockjaw peptide from *Conus purpurascens* venom. Biochemistry 34(15): 4913-4918.

Shon K, Stocker M, Terlau H, Stühmer W, Jacobsen R, Walker C, Grilley M, Watkins M, Hillyard DR, Gray WR, Olivera BM. 1998. κ-Conotoxin PVIIA: a peptide inhibiting the *Shaker* κ^+ channel. J Biol Chem. 273(1): 33-38.

Smith NJ, Hone AJ, Memon T, Bossi S, Smith TE, McIntosh JM, Olivera BM, Teichert RW. 2013. Comparative functional expression of nAChR subtypes in rodent DRG neurons. Front Cell Neurosci. 7:225.

Teichert RW, Smith NJ, Raghuraman S, Yoshikami D, Light AR, Olivera BM. 2012. Functional profiling of neurons through cellular neuropharmacology. Proc Natl Acad Sci. 109(5): 1388-1395.

Terlau H, Olivera BM. 2004. *Conus* venoms: A rich source of novel ion channel-targeted peptides. Physiol Rev. 84(1): 41-68.

Terlau H, Shon K, Grilley M, Stocker M, Stühmer W, Olivera BM. 1996. Strategy for rapid immobilization of prey by a fish-hunting cone snail. Nature 381(6578): 148-151.

Walker C, Steel D, Jacobsen R, Lirazan M, Cruz L, Hooper D, Shetty R, Dela Cruz R, Nielsen J, Zhou LM, Bandyopadhyay P, Craig AG, Olivera BM. 1999. The T-superfamily of conotoxins. J Biol Chem. 274(43): 30664 – 30671.

Williams JA, Day M, Heavner JE. 2008. Ziconotide: An update and review. Expert Opin Pharmacother. 9(9): 1575-1583.

Wilson MJ, Zhang MM, Gajewiak J, Azam L, Rivier J, Olivera B, Yoshikami D. 2015. α- and β-subunit composition of voltage-gated sodium channels investigated with μ-conotoxins and the recently discovered μO§-conotoxin GVIIJ. J Neurophysiol. 113(7): 2289-2301.

Wolfender JL, Chu F, Ball H, Wolfender F, Fainzilber M, Baldwin MA, Burlingame AL. 1999. Identification of tyrosine sulfation in *Conus pennaceus* conotoxins α-PnIA and α-PnIB: further investigation of labile sulfo- and phosphopeptides by electrospray, matrix-assisted laser desorption/ionization (MALDI) and atmospheric pressure MALDI mass spectrometry. J Mass Spectrom. 34(4): 447-454.

Woodward S, Cruz L, Olivera B, Hillyard D. 1990. Constant and hypervariable

regions in conotoxin propeitdes. EMBO J. 9(4): 1015-1020.

Zhangsun D, Luo S, Wu Y, Zhu X, Hu Y, Xie L. 2006. Novel O-superfamily conotoxins identified by cDNA cloning from three vermivorous Conus species. Chem Biol Drug Des. 68(5): 256-265.

CHAPTER 2

T- SUPERFAMILY CONOTOXINS FROM MOLLUSK-HUNTING CONE SNAILS: BIOLOGICAL ACTIVITY AND INHIBITION OF THE NOREPINEPHRINE TRANSPORTER (NET)

Abstract

In this paper we report three vertebrate-active conotoxins purified from mollusk-hunting cone snails. These conotoxins belong to the T-superfamily and have the cysteine framework I (-**CC**XXXX**C**XO**C**-). Two conotoxins χ-AuId from *Conus aulicus* and χ-AoIc from *Conus araneosus* inhibit NET with IC_{50}'s of 2.6 (± 0.4) μM and 0.7 (± 0.2) μM, respectively. The conotoxin fv1a from *Conus furvus*, although sharing 67% sequence identity with the NET-inhibiting conotoxins, did not inhibit NET, thus making it possible to identify residues that are functionally critical for NET inhibition. Interestingly, fv1a displayed activity in calcium imaging assays of dissociated dorsal root ganglion (DRG) neurons and upon intracranial (IC) injection into mice. We interpret these results to mean that a signaling molecule other than NET is an alternate target of conopeptides with a cysteine scaffold shared by χ-MrIa, χ-AuId, χ-AoIc, and fv1a. The discovery and characterization of these conotoxins suggest that: 1) the clade of mollusk-hunting cone snails contains a huge repository of compounds that inhibit NET, and 2) there is functional diversity within this group of homologous conotoxins expressed by the mollusk-hunters.

Introduction

The cone snails are venomous marine animals that inhabit tropical oceans. Based on predation behavior, the cone snails can be classified into three major groups: fish hunters (piscivores), mollusk hunters (molluscivores), and worm hunters (vermivores) (Kohn 1959; McIntosh and Jones 2001; Olivera et al.

1990; Olivera 1997). The vermivores are the largest group and probably retains the ancestral trait. There are ~850 species of cone snails and all of them use venom to capture their specific prey (Favreau and Stocklin 2009; Olivera 2002; Röckel et al. 1995). The cone snail venom primarily contains small peptidic molecules called conopeptides/conotoxins (Olivera et al. 1990; Olivera et al. 1985; Teichert et al. 2015; Terlau and Olivera 2004).

The conotoxins are gene products that are initially translated as a precursor (Buczek et al. 2005; Olivera 1997) with three regions: the signal sequence at the N-terminus, an intervening propeptide region, and the mature toxin region at the C-terminus (Colledge et al. 1992; Robinson and Norton 2014). Conotoxins that share a highly conserved signal sequence and a characteristic pattern of cysteine residues in the toxin region belong to a conotoxin superfamily (Terlau and Olivera 2004; Woodward et al. 1990). Members of a superfamily with the same biological target are further grouped into pharmacological families (Terlau and Olivera 2004).

The T-superfamily is one of these conotoxin superfamilies and is widely expressed in cone snails across all feeding groups (Walker et al. 1999). The conotoxins in this superfamily are small (11 – 17 amino acids) and are structurally stabilized by two disulfide bonds (Walker et al. 1999). Members of the T-superfamily fall into two groups based on the framework of cysteine residues in the toxin region. One group has the cysteine framework V (CC-CC) (Terlau and Olivera 2004, Walker et al. 1999) while another group which includes the χ-conotoxins has the cysteine framework I (CC-CXOC) (Terlau and Olivera 2004,

Walker et al. 1999). One member of the T-superfamily, the conotoxin χ-MrIA from *Conus marmoreus* was shown to inhibit the norepinephrine transporter (NET) (Sharpe et al. 2001). χ-MrIA has the cysteine framework I and is the founding member of the χ-conotoxin family in the T-superfamily.

To our knowledge, χ-MrIA has been the only conotoxin reported to inhibit NET, and hence, the only known member of the χ-conotoxin family (Balaji et al. 2000; McIntosh et al. 2000; Sharpe et al. 2001). χ-MrIA has been shown to be antinociceptive (McIntosh et al. 2000) and is currently undergoing clinical trials for the treatment of pain (Brust et al. 2009; Green et al. 2014). χ-MrIA was purified from the mollusk hunter *C. marmoreus*. We therefore reasoned that other mollusk-hunting cone snails potentially express conotoxins homologous to χ-MrIa. The method of phylogeny-assisted conotoxin discovery has been successfully used in the search of novel conotoxins with specific activity (Azam and McIntosh 2009: Bulaj 2008; Espino et al. 2016; Olivera 2006; Olivera and Teichert 2007; Platt et al. 2014).

In the search for novel conotoxins that inhibit NET, we focused on three species from the different clades of mollusk-hunting cone snails namely: *Conus aulicus* (*Darioconus* clade), *Conus araneosus* (*Conus* clade), and *Conus furvus* (*Calibanus* clade) (Figure 2.1) (Puillandre et al. 2014). In this paper, we identified and characterized the biological activities of three conotoxins belonging to the T-superfamily. The pattern of cysteine residues indicates that these conotoxins belong to cysteine framework I. Bioactivity-guided purification identified the NET-inhibiting conotoxin, χ-AuID, from the venom of *Conus aulicus*. A publication by

Gupta et al. (2010) identified the conotoxin Ar1311 from *Conus araneosus* which has the cysteine framework I. Our assay revealed that this conotoxin also inhibits the activity of NET. The third conotoxin, fv1a, a component of one of the major HPLC peaks in the *C. furvus* venom did not inhibit NET, but elicited cellular response monitored by calcium imaging of mouse dorsal root ganglion (DRG) neurons and induced aberrant behavior in mice upon intracranial (IC) injections. The conotoxins we report in this paper all have the cysteine framework I, however, the activities of these conotoxins are divergent indicating functional diversity of framework I conotoxins in the T-superfamily.

Materials and methods

Extraction and fractionation of crude venom. Lyophilized venom (550 mg) from *Conus aulicus* collected from the Philippines was extracted with 40 mL of a solution containing 40% acetonitrile (ACN) and 0.1% trifluoroacetic acid (TFA). The suspension was vortexed for 1 min and homogenized in a 50 mL glass-teflon homogenizer (5 cycles at 13,000 x g). The homogenate was vortexed for 10 s and centrifuged at 27,000 rpm for 10 min. The supernatant was diluted with a solution containing 0.1% TFA and applied on a preparative HPLC column. The components of the venom were eluted using a linear gradient of buffers consisting of 0.1% TFA (buffer A) and 90% ACN in 0.082% TFA (buffer B90).

Conus furvus snails were purchased from a fish market in Guimaras Island, Philippines. The venom duct was dissected from 50 snails and the venom

was manually squeezed (in ice) out of the ducts and lyophilized. A 20-mg portion of the lyophilized venom was extracted with 1 mL solution containing 30% ACN and 0.1%TFA. The suspension was kept in ice and homogenized by vortexing every 10 min. After 30 min, the suspension was centrifuged at 13,000 x *g* for 15 min and the supernatant was separated from the pellet. The extraction was repeated two more times and the supernatants from the three extractions were pooled and diluted to 3 times of the original volume with 0.1% TFA. This solution was then fractionated on Vydac C_{18} semipreparative column (5 μm, 10mm x 250 mm). The venom components were eluted using a linear gradient by mixing 0.1% TFA (Buffer A) and 90% ACN in 0.1% TFA (Buffer B90). The absorbance at 220 nm was monitored and individual peaks corresponding to individual fractions were collected.

Purification of conotoxins from *C. aulicus and C. furvus*. The peptides from *C. aulicus*, and *C. furvus* were further purified by analytical reverse phase chromatography using a Vydac C_{18} monomeric column (5 μm, 4.6 mm x 250 mm). Separation of components contained in the norepinephrine-transporter-inhibiting fraction obtained by preparative HPLC of *C. aulicus* venom was accomplished using a linear gradient constructed by mixing 30% - 50% Buffer B90 with Buffer A over the course of 20 min at a flow rate of 1 mL/min. Sample homogeneity was verified by secondary analytical HPLC applying the same gradient as the semipreparative HPLC. Major components in the *C. furvus* venom were purified by analytical HPLC. The conotoxin fv1a was one of the major component and was purified using a gradient of 10% - 30% B90 over 20

min at a flow rate of 1 mL/min. The purity of fv1a was verified by secondary analytical HPLC applying the same gradient.

Reduction and alkylation of the purified peptides. Purified peptides from *C. aulicus*, and *C. furvus* were reduced using dithiothreitol (DTT) and alkylated using 4-vinylpyridine (4-VP). In these reactions the pH was buffered to pH 8 using 0.5 M Tris base, reductant was added to a final concentration of 10 mM DTT and the temperature was maintained a 65 ºC for 30 min. Subsequent alkylation was initiated by adding 0.8 μL of 4-VP and proceeded in the dark, at room temperature, for 30 min. The reduced and alkylated peptide was purified from the reaction using an analytical reverse-phase HPLC column.

Peptide sequencing. Approximately 70 pmol of the alkylated peptide was sequenced by Edman degradation at the the DNA/peptide core facility, University of Utah. The 3-phenyl-2-thiohydantoin amino acid derivatives were identified by HPLC.

Mass spectrometry. MALDI mass analysis was performed using the Applied Biosystems Voyager System 4271 scanning over the *m/z* range between 0.7 – 3 kDa in the reflector mode.

Identification and sequencing of clones encoding *Conus aulicus* χ-AuID. cDNA from *C. aulicus* was used as a template for polymerase chain reaction (PCR) with oligonucleotides corresponding to conserved regions of the signal sequence and 3' UTR sequences of Chi-prepropeptides. The resulting PCR products were purified using the High Pure PCR Product Purification Kit (Roche Diagnostics, Indianapolis, IN) following the manufacturer's suggested

protocol. The eluted DNA fragments were annealed to pAMP vector using the CloneAmp pAMP System for Rapid Cloning of Amplification Products (Life Technologies/Gibco BRL, Grand Island, NY) following manufacturer's suggested protocol and the resulting products transformed into DH5α competent cells. The nucleic acid sequences of these Chi-encoding clones were determined according to the standard protocol for automated sequencing.

Identification and sequencing of clones encoding *Conus furvus* fv1a. cDNA from *Conus furvus* was used as a template for polymerase chain reaction (PCR) with oligonucleotides corresponding to conserved regions of the signal sequence and 3' UTR sequences of Chi-prepropeptides. The resulting PCR products were purified using the High Pure PCR Product Purification Kit (Roche Diagnostics, Indianapolis, IN) following the manufacturer's suggested protocol. The eluted DNA fragments were annealed to pNEB206A vector using the USER Friendly Cloning kit (NewEngland BioLabs, Inc., Beverly, MA) following manufacturer's suggested protocol and the resulting products transformed into DH5α competent cells. The nucleic acid sequences of these Chi-encoding clones were determined according to the standard protocol for automated sequencing.

Peptide synthesis. The peptide χ-Au1D was synthesized at the DNA/Peptide Facility at the University of Utah. The peptides fv1a and Ar1311 were synthesized with an Apex 396 automated peptide synthesizer (AAPPTec, Louisville, KY) using a standard solid-phase Fmoc (9-fluorenylmethyloxycarbonyl) protocol. Ar1311 (χ-AoIC) was syntheseized on Fmoc-L-Cys(Acm)-Wang resin (substitution: 0.55 mmolg-1, Peptides

International Inc, Louisville, KY) and Fv1a on Fmoc-L-Pro-2-Cl-Trt resin(substitution: 0.9 mmolg-1, AAPPTec, Louisville,KY). All standard amino acids were purchased from AAPPTec and N-α-Fmoc-(O-tBu)-L-trans-4-hydroxyproline form NovaBiochem (Merck KGaA, Darmstadt, Germany). Side-chain protection for the following amino acids was: Asp and Hyp: O-tert-butyl (OtBu); Arg: 2,2,4,6,7-pentamethyldihydrobenzofuran-5-sulfonyl (Pbf), Lys: tert-butyloxycarbonyl (Boc); Tyr and Thr: tert-butyl (tBu); His: trityl (Trt). In order to control oxidative folding of the cysteines, orthogonal protection was used: one pair of Cys (Cys 1 and Cys 4) was Trt protected; the second pair (Cys 2 and Cys 3) was protected with *acetamidomethyl* (Acm) group. Peptides were synthesized on 50 μmol scale. Coupling activation was achieved with one equivalent of 0.4 M benzotriazol-1-yl-oxytripyrrolidinophosphonium hexafluorophosphate (PyBOP) and two equivalents of 2 M *N,N*-diisopropylethyl amine (DIPEA) in *N*-methyl-2-pyrrolidone (NMP) and ten-fold excess of amino acid. Each coupling reaction was conducted for 60 min. Fmoc deprotection reaction was carried out for 20 min with 20% piperidine in DMF.

Oxidative folding of the linear peptides. The linear peptide was cleaved from 25 mg of resin using 1 mL reagent K (11.0 M TFA, 3.0 M ethanedithiol (EDT), 4.0 M thioanisole (TIS) and 0.5 M phenol), and precipitated in ice-cold methyl *tert*-butyl ether (MTBE). After the removal of MTBE, the precipitate was resuspended in buffer A (0.1% TFA) and purified using a Vydac C_{18} semipreparative reverse-phase column. Peptide folding was achieved in two steps. The first disulfide bridge was formed by incubating the linear peptide in a

solution containing 1.0 mM GSSG, 2.0 mM GSH, 100 mM Tris (pH = 7.5) and 0.1 mM EDTA for 2 h. The folded peptide was separated from the solution by semipreparative HPLC. The formation of the second disulfide bridge was achieved by incubating the peptide for 20 min in a solution containing 24% ACN (v/v), 380.0 mM TFA and 5.0 mM I_2. The folded peptide was purified by reverse phase analytical chromatography on a C_{18} HPLC column. The identity of the folded peptide was confirmed by mass spectrometry and co-elution with the native peptide isolated from venom.

Cell culture. Human embryonic kidney cells stably expressing the human norepinephrine transporter (HEK293-hNET) were grown in Dulbecco's modified Eagle's media containing 10% (v/v) FBS, 100 units/mL penicillin, 100 μg/mL streptomycin, 2 mM L-glutamine, and 250 μg/mL G418 at 37 ^{0}C and 5% CO_2 in a humidity controlled incubator.

Norepinephrine uptake assay. The norepinephrine uptake assay followed the protocol described in Galli et al. (1995). HEK293-hNET cells were plated at a density of approximately 50,000 cells/well on an amine coated 96-well tissue culture plates 1 day before the experiment. On the day of the experiment, the medium was aspirated and the cells washed once with Krebs-Ringer's-HEPES (KRH) buffer (130 mM NaCl, 1.3 mM KCl, 2.2 mM $CaCl_2$, 1.2 mM $MgSO_4$, 1.2 mM KH_2PO_4, 10 mM HEPES, 1.8 g/L dextrose, pH 7.4). The cells were preincubated with the conotoxins for 10 min at 37 ^{0}C in KRH buffer supplemented with 100 mM L-ascorbate, 100 mM pargyline, and 10 mM U-0521(catechol *O*-methyl transferase inhibitor). Uptake assay was initiated by the

addition of norepinephrine, Levo-[ring-2, 5, 6-^{3}H] to a final concentration of 50 nM. The uptake assay was performed at 37 ^{0}C for 15 min and terminated by rapid aspiration of the uptake buffer followed by 2 washes with 200 μL ice-cold KRH buffer. The cells were then lysed with 100 μL of a 10% SDS solution at room temperature with gentle shaking for 60 min. Accumulated radioactivity in the 50 μL of the lysate was measured using liquid scintillation spectrometry. The remaining 50 μL of the lysate was used to measure protein concentration using the DC protein assay kit (BioRad), following the manufacturer's protocol. A parallel experiment was performed in the presence of 1.0 μM desipramine to account for nonspecific uptake.

Mouse bioassay. Experimental protocols for experiments involving live animals were approved by the Institutional Animal Care and Use Committee (IACUC) of the University of Utah. Mice (17 – 21 days) were injected intracranially (IC) with peptide in 10 μL saline solution. Mice were observed for aberrant behavior for 3 h.

Calcium imaging assay. Experimental protocols for experiments involving live animals were approved by the Institutional Animal Care and Use Committee (IACUC) of the University of Utah. Dissection of the dorsal root ganglia (DRG) was done following previously described protocols (Teichert et al. 2012; Smith et al. 2013). Lumbar DRG neurons from wild type C57/BL6 mouse were dissociated, pooled, and cultured overnight for calcium imaging experiments. Cells were loaded with Fura-2-AM dye one hour before the experiment. During the experiment, the dye inside the cells was excited

alternately with 340 nm and 380 nm light. The ratio of the emission 510 nm from both excitations was measured. The ratio of the fluorescence intensity is a measure of the increase in intracellular calcium resulting from the depolarization caused by the external application of 25 mM KCl. KCl was applied every 7 min. After the third KCl pulse, 1.5 μM fv1a was applied and its effects on the levels of intracellular calcium were monitored.

Results

Purification, characterization and sequencing of a χ-conotoxins from *C. aulicus*. High performance liquid chromatography (HPLC) purification of χ-AuID was achieved by following its activity to inhibit the reuptake of norepinephrine (NE) via the human norepinephrine transporter (hNET) heterelogously expressed in human embryonic kidney (HEK) cells. Fractions from the semipreparative HPLC (Figure 2.2A) of the crude *Conus aulicus* venom were screened for activity against NET. The active fraction was further purified to homogeneity by analytical HPLC (Figure 2.2B-C).

Matrix-assisted laser desorption ionization (MALDI) mass analysis of the active homogeneous sample revealed a single peptide with a mass of 1332.4 Da. The reduced and alkylated peptide has a mass of 1752.6 Da. The change in mass can be attributed to the alkylation of four cysteine residues by 4-vinylpyridine (105 Da). Edman chemical analysis revealed a 12 amino acid peptide with the sequence SVCCGYKLCFOC where O indicates a proline post-translationally modified to a hydroxyproline. The mass predicted from this

sequence is 1333.6 Da which differs by +1.2 Da from the mass of the native peptide obtained by MALDI mass analysis, suggesting the posttranslational modification of the peptide C-terminus into an amide. These results are consistent with the peptide sequence: SVCCGYKLCFOC-NH_2 (Table 2.1). Since this peptide inhibits NET, we propose to call this peptide χ-AuId following the nomenclature for naming conotoxins (Olivera and Cruz 2001).

Purification, characterization, and sequencing of fv1a. Purification of the major HPLC fractions in the venom of *Conus furvus* led to the identification of the conotoxin fv1a (Figure 2.3A-C). MALDI mass analysis revealed the mass of the native peptide to be 1286.4 Da. Edman chemical analysis determined the sequence to be: GVCCAHTGCKOCP (Table 2.1) where O is a hydroxyproline residue. The predicted mass of this sequence is 1286.5 Da in agreement with the experimental mass of the native peptide measured by MALDI-MS and indicating the C-terminus is unmodified. A comparison of the fv1a sequence with those of the χ-conotoxins (Table 2.1) revealed a conserved pattern of cysteine residues and a conserved loop size between the cysteine residues.

Peptide synthesis and folding. The correctness of the sequence assignment of χ-AuID and fv1a was verified by HPLC co-elution experiments of the synthetic and venom-derived peptides. The linear peptides were oxidatively folded, and the major components from these folding reactions were purified to >99% homogeneity. MALDI mass analysis of the products of the folding reactions revealed a mass of 1322.5 Da for the synthetic χ-AuID and a mass of 1286.4 Da for the synthetic fv1a. The synthetic χ-AuID and fv1a each co-eluted with their

corresponding native peptides (Figure 2.4). These results verify the sequence assignments for χ-AuID and fv1a and demonstrate that each mature toxin is able to correctly fold without assistance if provided with an appropriate redox environment. Folding instructions are thus intrinsic to the mature toxin sequence and not inscribed in the propeptide.

Ar1311 was synthesized following the sequence and disulfide connectivity determined by Gupta et al. (2010). In the paper the peptide was reported to have the sequence: RCCGYKMCHOC (Table 2.1) and stabilized by disulfide bonds between Cys1 and Cys4 and between Cys2 and Cys3. The linear Ar1311 was oxidatively folded and the major component was purified to >99% homogeneity. MALDI mass analysis of the folding reaction product yielded a mass of 1311.3 Da which is consistent with the reported mass of the peptide.

NET uptake assay. Ar1311 was previously identified by Gupta et al. (2010) using mass spectrometric methods. The sequence of this peptide is shown in Table 2.1. The amino acid sequence of Ar1311 shows a high degree of similarity with the amino acid sequence of χ-conotoxins, thus Ar1311 is a potential NET antagonist. Ar1311 was synthesized and tested for activity against NET. Results from the assay showed that Ar1311 inhibits the activity of the transporter (Figure 2.5). Since Ar1311 has the same pharmacological activity as the χ-conotoxins we propose to rename this peptide χ-AoIC following the rules for naming conotoxins (Olivera and Cruz 2001). The conotoxin fv1a failed to show any activity even at concentrations as high as 200 μM (Figure 2.5). The result of the fv1a experiment suggested that NET is not the molecular target of

fv1a.

Further characterization of the activity of both χ-AoIC and χ-AuID against NET showed that these peptides inhibit the transporter in a dose-dependent manner (Figure 2.5). Experiments using increasing concentrations of χ-AuID and χ-AoIC were performed to determine the concentration of conotoxin required to inhibit 50% of transporter activity (IC_{50}). These experiments showed the IC_{50} of χ-AoIC to be 0.7 ± 0.2 μM and that of χ-AuID to be 2.6 ± 0.4 μM. The alignment of the sequences of χ-AuID, χ-AoIC and the previously identified NET inhibitor χ-MrIA, a conotoxin that belongs to the T-superfamily (McIntosh et al. 2000) revealed a striking conservation in the amino acid sequences of the conotoxins especially in the region between Cys2 and Cys3 (Table 2.1). These peptides share identical pharmacology hence fall under the χ-conotoxin family in the T-superfamily.

cDNA cloning and precursor sequence of fv1a and χ-AuID. Conotoxin fv1a did not inhibit NET, and is thus pharmacologically different from the χ-conotoxins, however, the conserved arrangement of cysteine residues in these peptides suggests that fv1a belongs to the same conotoxin superfamily as χ-AuID and χ-AoIC. Conotoxins that belong to the same superfamily have a highly conserved signal sequence as well as conserved pattern of cysteine residues in the toxin region. Therefore, we determined the precursor sequences of fv1a and χ-AuId to rigorously test the hypothesis that fv1a belongs in the same superfamily as the χ-conotoxins.

The cloned cDNA sequences encoding precursors of χ-AuID and fv1a

displayed the canonical organization typical for a conotoxin precursor (Figure 2.6). As expected, the signal sequences found at the predicted N-terminus are composed primarily of hydrophobic amino acids. The signal sequence is followed by the pro-region and the toxin coding region is found at the C-terminal. The position corresponding to the hydroxyprolines in χ-AuID and fv1a is expectedly occupied by prolines in the clones. Moreover the C-terminal of the χ-AuID precursor contains a glycine residue. The presence of C-terminal glycine is expected since it was shown that the native χ-AuId is amidated at the C-terminal. The C-terminal glycine in conotoxins is posttranslationally modified into an amide (Ul-Hasan et al. 2013).

Sequence alignment of the precursors of fv1a, χ-AuID, and χ-MrIA (Figure 2.6) revealed that that only 8 of the 24 amino acids in the signal sequence are not conserved. This high degree of conservation of amino acids in the signal sequence indicates that fv1a like the χ-conotoxins is a member of the T-superfamily. The conclusion that fv1a belongs to the T-superfamily is further supported by the conserved pattern of cysteine residues between fv1a and χ-conotoxins.

Biological activity of fv1a. Two assays tested whether fv1a exhibits biological activity in mice. One assay followed the behavior after intracranial (IC) injection. The other assay measured changes in intra-cellular calcium ion concentration of dissociated mouse dorsal root ganglion (DRG) neurons following membrane depolarization (Figure 2.7).

IC injection of fv1a caused a hyperactive phenotype in young mice (17 –

21 day old). The hyperactive behavior was manifested by the animals running, climbing and jumping in cages. Interestingly, peptide doses as low as 0.1 nmol elicited this hyperactive behavior. Control subjects showed no difference in behavioral activity following IC injection of saline. In comparison, χ-MrIA causes a sluggish phenotype in mice (McIntosh et al. 2010) while a related peptide, CTMrVIA that lacks the first two amino acids of χ-MrIA at the N-terminus, causes seizures and death in mice (Balaji et al. 2000). Calcium imaging of dissociated DRG neurons in the presence of 1.5 μM fv1a resulted in partial inhibition of intracellular calcium increase upon depolarization using 25 mM KCl (Figure 2.7). A similar concentration of the χ-conotoxins potentiates the calcium response upon depolarization using 25 mM KCl (Figure 2.7). The behavioral and cellular responses resulting from the application of fv1a suggest that the peptide acts on a component of the mouse nervous system. Since fv1a does not inhibit NET *in vitro* and elicits behavioral and cellular responses that are different from the behavioral and cellular responses elicited by the χ-conotoxins, we conclude that the molecular target of fv1a is different from the target of χ-conotoxins.

Discussion

Phylogeny-directed discovery has been successfully employed in the search of conotoxins with novel pharmacological properties (Azam and McIntosh 2009; Bulaj 2008; Espino et al. 2016; Olivera 2006; Olivera and Teichert 2007; Platt et al. 2014). The information inferred from phylogenetic relationships among cone snails aided in the discovery of three conotoxins namely: χ-AuId, χ-AoIc,

and fv1a. These conotoxins were purified from the venom of mollusk-hunting cone snails *C. aulicus* (χ-AuID), *C. araneosus* (χ-AoIC), and *C. furvus* (fv1a). In this study, we investigated whether different groups of mollusk-hunting snails express conotoxins that inhibit the reuptake of norepinephrine (NE) through the norepinephrine transporter (NET). Previously it had been shown that a mollusk-hunter (*C. mamoreus*) expresses the conotoxin χ-MrIa which inhibits the reuptake of NE via NET (Sharpe et al. 2001). We hypothesized that other mollusk-hunting snails also express conotoxins that inhibit NET. Our hypothesis was validated when the NET-inhibiting conotoxins χ-AuID and χ-AoIC were identified from the venom of *C. aulicus* and *C. araneosus,* respectively. Surprisingly, the conotoxin fv1a did not inhibit the activity of NET although it appears to be related to the χ-conotoxins. The conotoxin fv1a is biologically active when injected intracranially (IC) into mice and in the calcium imaging of dissociated mouse dorsal root ganglion (DRG) neuron.

The conotoxins χ-AuID and χ-AoIC share the same pharmacological activity and are members of the χ-conotoxin family. The χ-conotoxins belong to the larger T-superfamily. The conotoxin fv1a shares the same cysteine framework as the χ-conotoxins. Moreover, analysis of the precursor sequence of fv1a and χ-AuID revealed a very high degree of similarity of the amino acids in the signal sequence. These results indicate that fv1a is also a member of the T-superfamily. fv1a does not inhibit NET however the *in vivo* activity of this conotoxin in mice and its inhibition of the cytosolic influx of calcium in response to the application of high external $[K^+]_o$ indicate that the target of this peptide is

biologically relevant in mammals. The characterization of the conotoxins reported in this paper indicates the diversity in the biological activity of framework I conotoxins in the T-superfamily. The conotoxin fv1a could potentially define a new family in the T-superfamily with a unique biological and pharmacological activity.

The inability of fv1a to inhibit NET allowed the opportunity to perform a nature-designed structure activity relationship (SAR) studies to identify amino acids critical for the inhibition of NET. A comparison of fv1a, χ-AuIdD, χ-AoIC, and χ-MrIA sequences (Table 2.1) revealed that the amino acids in the first loop between the second cysteine (Cys2) and the third cysteine (Cys3) are highly divergent between NET inhibitors and non-NET inhibitors (e.g., between χ-AuID and fv1a) whereas the same region is conserved between conotoxins that inhibit NET (e.g., χ-AuID and χ-AoIC). Conservative amino acid substitution in the region between Cys2 and Cys3 is tolerated. For example, a substitution of the leucine residue in χ-AuID with a methionine in χ-AoIC did not affect the ability of these peptides to inhibit NET. These observations suggest that the amino acids between Cys 2 and Cys 3 are important determinants for activity against NET. Changes in the second loop between Cys3 and Cys4 do not appear to affect NET activity as demonstrated by χ-AuID and χ-AoIC. The results of the natural χ-conotoxin SAR are similar to those obtained from the SAR studies of χ- MrIA (Brust et al. 2009).

The framework I conotoxins in the T-superfamily appear to be restricted to mollusk-hunting cone snails. A systematic screen (unpublished data) of cone

snails across different clades identified these conotoxins only in mollusk-hunters. It is highly probable that these conotoxins are important for prey capture. The χ-conotoxins, for example, are possibly used in predation through the perturbation of noradrenergic signaling in their molluskan prey since norepinephrine acts as a neurotransmitter in mollusks (Adamo 2008; Lacoste et al. 2001; Sloley et al. 1990). The conotoxins reported in this paper suggest that the clade of mollusk-hunting cone snails contains a huge repository of compounds that inhibit NET. Thus, it is important for continued research on this group of cone snails to discover more NET-inhibiting conotoxins. These conotoxins would prove useful in research and medicine.

The reuptake of norepinephrine through NET is the mechanism which terminates noradrenergic signaling. NET has been implicated in various neuorological conditions and compounds that target NET have been developed as drugs for the treatment of diseases such depression, attention-deficit hyperactivity disorder (ADHD), eating disorders, and pain (Bönisch and Brüsss 2006; Zhou 2004). Thus, the χ-conotoxins are important leads for the development of better drugs for the treatment of the above mentioned pathological conditions. For example, the χ-conotoxin, χ-MrIa is undergoing clinical trials for the treatment of pain. The divergent activity of fv1a as opposed to the χ-conotoxins, as shown in the intracranial injections of the peptides, and in the calcium imaging of DRG neurons, indicates that there is a possible new conotoxin family in the T-superfamily and that this family contains conotoxins with a unique set of biological and pharmacological activities. Moreover, the activities

of these peptides in the calcium imaging experiments are particularly interesting. The molecular mechanisms underlying these observed activities will be the subject of future investigations.

Figure 2.1. **Phylogenetic relationships in mollusk-hunting cone snails**. The cone snail species from which conotoxins reported in this paper were isolated are shown in the right. These cone snails are *Conus aulicus*, *Conus araneosus,* and *Conus furvus*.

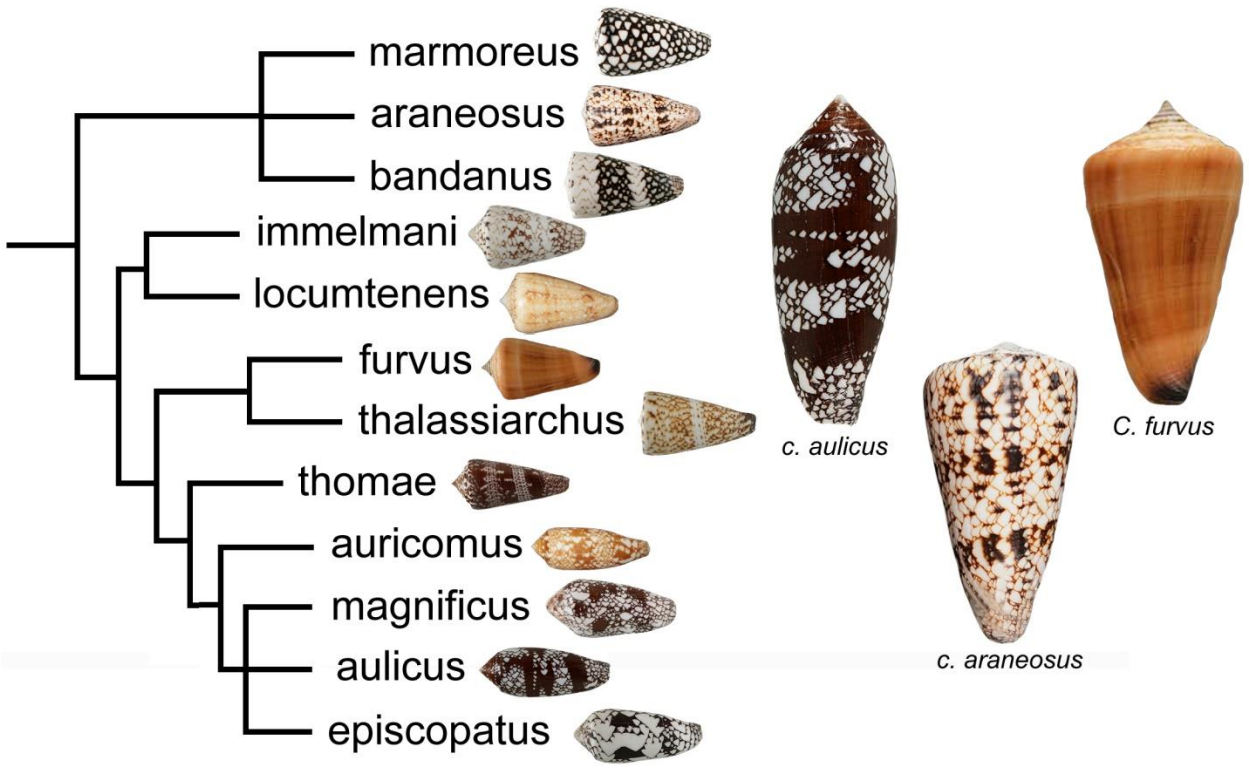
marmoreus
araneosus
bandanus
immelmani
locumtenens
furvus
thalassiarchus
thomae
auricomus
magnificus
aulicus
episcopatus
c. aulicus
c. araneosus
C. furvus

Figure 2.2. Purification of χ-Au1D. A) HPLC chromatogram showing the absorbance profile at 220 nm of crude *C. aulicus* venom fractionated on a preparative C_{18} column using a linear gradient of 1.3% B90/min at a flow rate of 20 mL/min. The fraction marked by the arrow showed inhibitory activity against NET. B) Analytical HPLC chromatogram profile of the subfractionation of the active component in A. The subfractionation was performed using a linear gradient of 30% - 50% B90 for 20 min at a flow rate of 1 mL/min. The active peak is marked by an arrow. C) Analytical HPLC chromatogram profile showing the homogeneity of the active fraction in B. The HPLC experiment was done using the same linear gradient described in B.

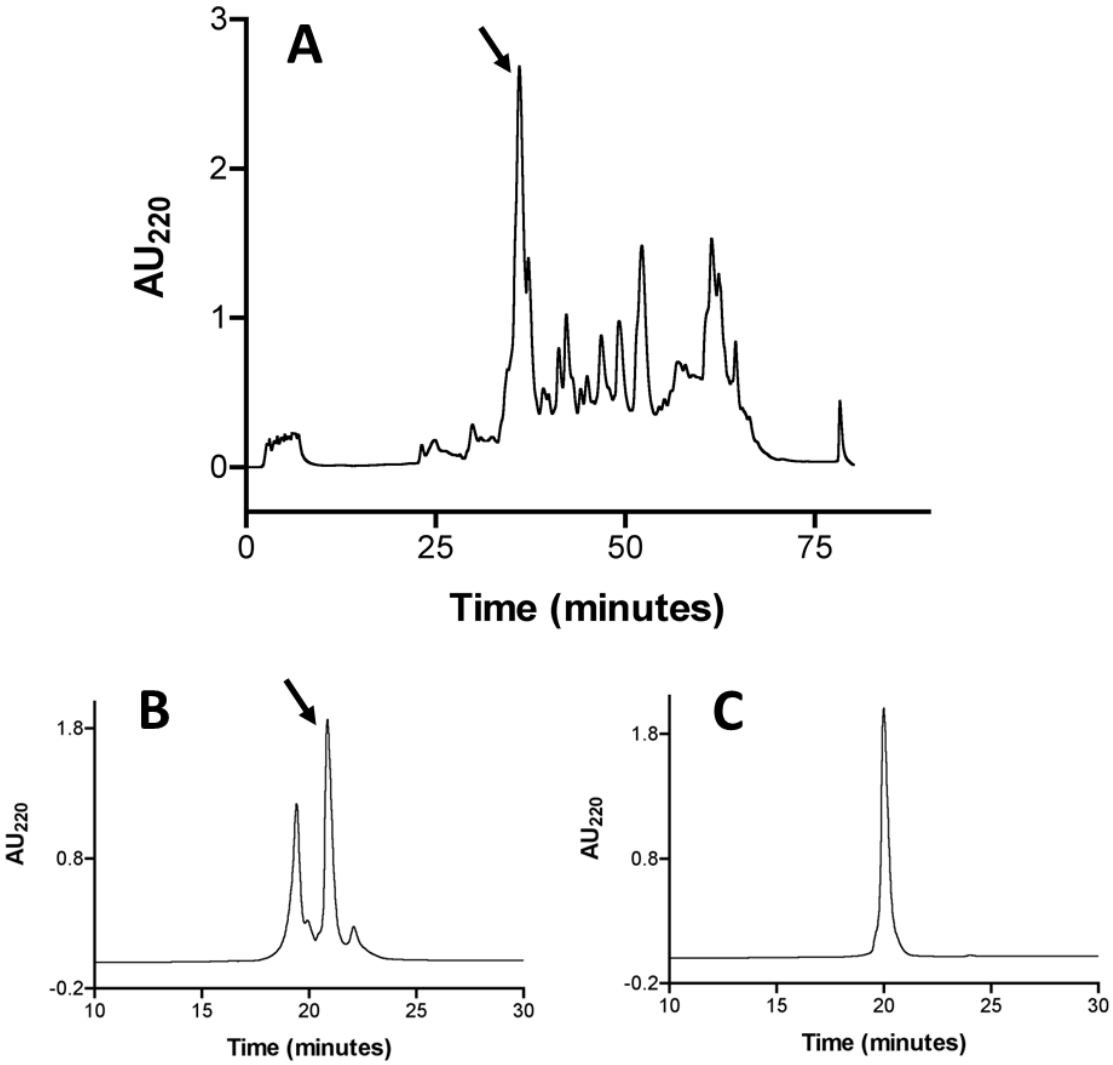
A
B
C
AU220
Time (minutes)
0
25
50
75
1
2
3
10
15
20
30
0.8
1.8
-0.2

Figure 2.3. Purification of fv1a. A) HPLC chromatogram showing the absorbance profile at 220 nm of crude *C. furvus* venom fractionated on a semi-preparative C_{18} column. The components were eluted using a gradient of 1.6% B90/min for 60 min at a flow rate of 4 mL/min. The HPLC peak marked by the arrow contains fv1a. B) Analytical HPLC profile of the subfractionation of the peak marked in A. The subfractionation experiment used a linear gradient of 1% B90/min starting at 10% B90 for 20 min. The arrow indicates the fraction containing fv1a. C) Analytical HPLC profile showing that fv1a has been purified to homogeneity. The gradient used to verify the purity of fv1a is the same gradient described in B.

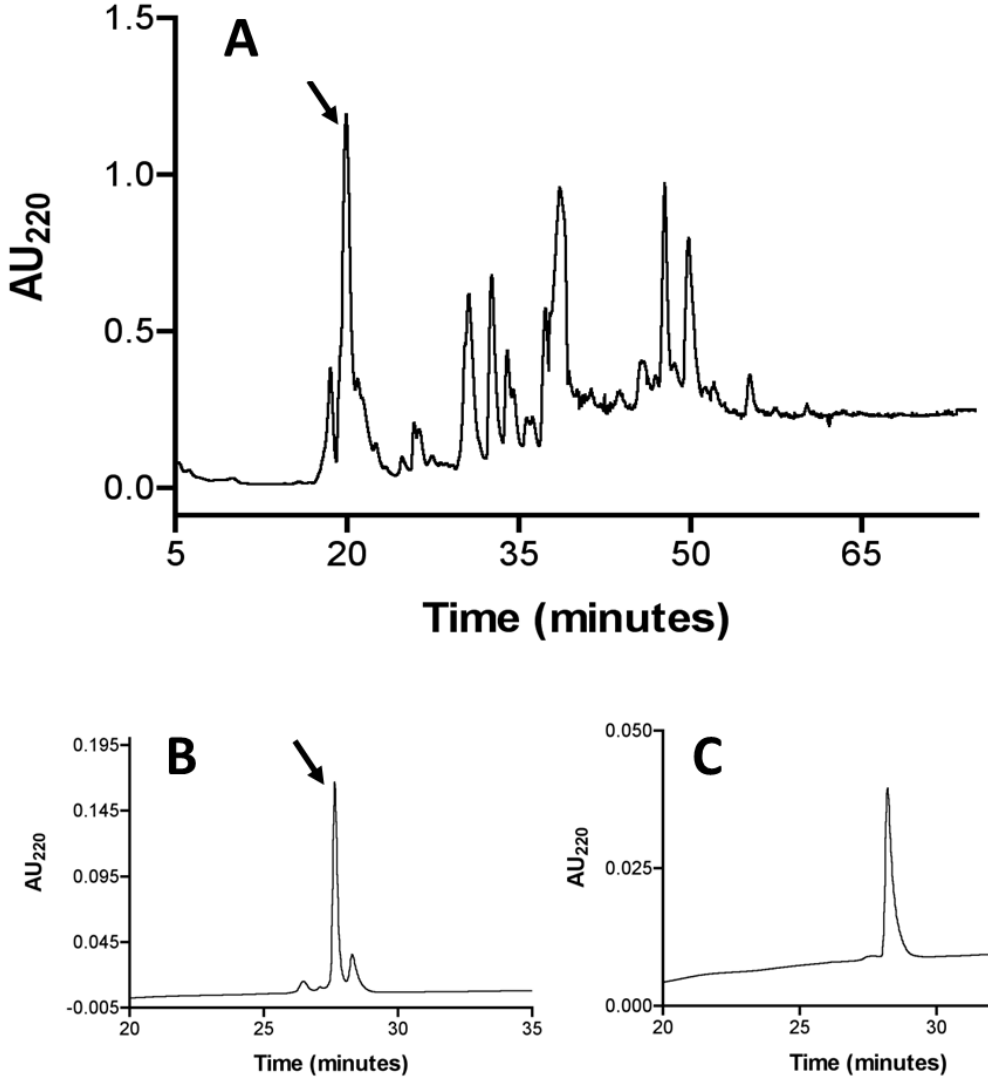
A
1.5
1.0
0.5
0.0
AU220
5
20
35
50
65
Time (minutes)
B
0.195
0.145
0.095
0.045
-0.005
AU220
20
25
30
35
Time (minutes)
C
0.050
0.025
0.000
AU220
20
25
30
35
Time (minutes)

Figure 2.4. Co-elution experiment of the native and synthetic χ-AuID and fv1a. The peptides were synthesized and folded as described in the "Experimental Procedures." A) Analytical HPLC chromatogram profile showing the absorbance at 220 nm of the native χ-AuId (top), synthetic χ-AuId (middle) and a mixture of the native and synthetic χ-AuId (bottom). The co-elution experiment was performed using a 1%/min linear gradient of B90 starting at 30% B90 for 20 min at a flow rate of 1 mL/min. B) Analytical HPLC chromatogram profile showing the absorbance at 220 nm of the native FvIa (top), synthetic fv1a (middle) and a mixture of the native and synthetic fv1a (bottom). The coelution experiment was perfromed using a linear gradient of 10% - 30% B90 for 20 min at a flow rate of 1 mL/min.

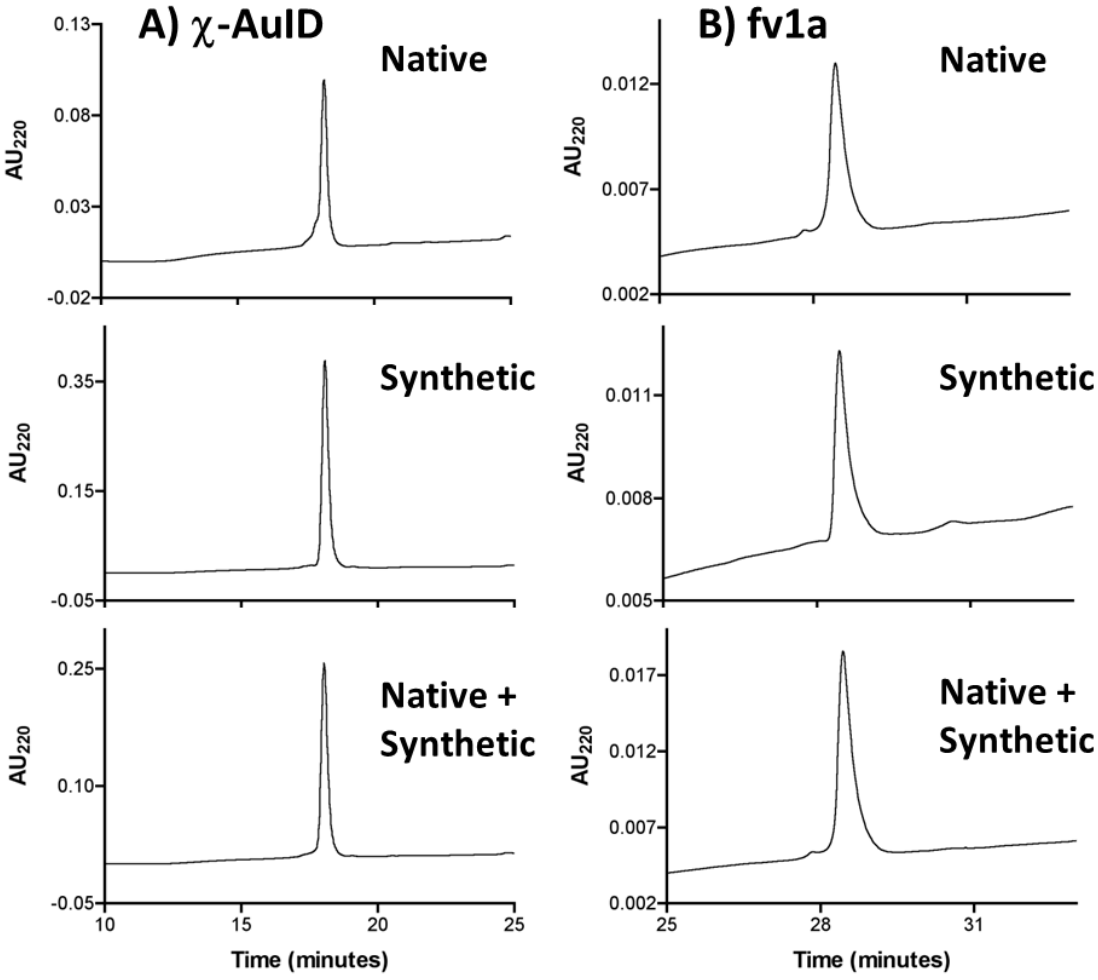
A) χ-AuID
Native
Synthetic
Native +
Synthetic
B) fv1a
Native
Synthetic
Native +
Synthetic
AU220
Time (minutes)

Figure 2.5. Activity of χ-AuID, χ-AoIC, and fv1a against human norepinephrine transporter (hNET) expressed in HEK-293 cells. The inhibitory activity of χ-AuID, and χ-AoIc against the human NET is dose-dependent. IC_{50} values for χ-Ao1C and χ-Au1d are 2.6 ± 0.4 μM and 0.7 ± 0.2 μM, respectively. The activity of fv1a against NET at 200 μM is also shown. Each data point was normalized against 100% activity occurring in the absence of the conotoxins. The IC_{50}'s are average values of three experiments performed in triplicates.

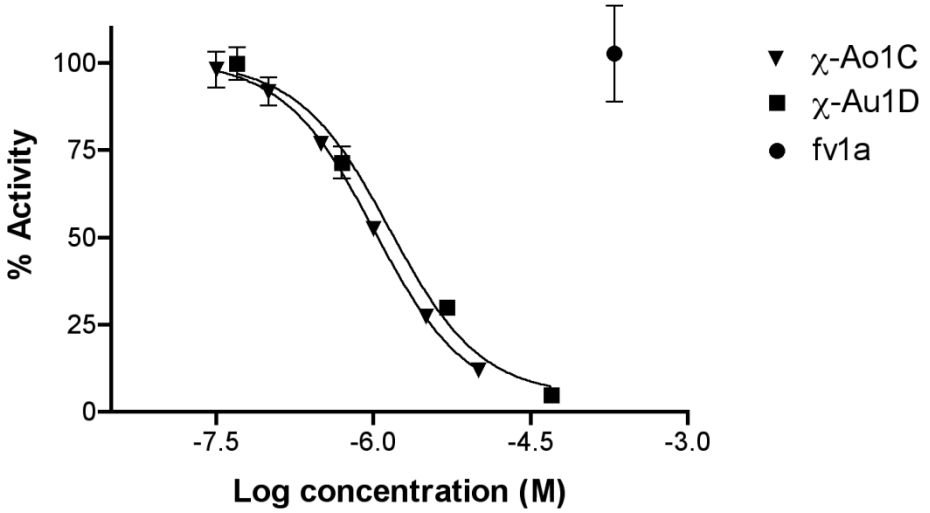
100
75
50
25
0
% Activity
-7.5
-6.0
-4.5
-3.0
Log concentration (M)
χ-Ao1C
χ-Au1D
fv1a

Figure 2.6. Sequence alignment of the precursors of fv1a, χ-AuID and χ-MrIA. These three precursors display a very high degree of sequence similarity in the signal sequence as well as a conserved pattern of cysteine residues in the toxin region indicating that these conotoxins belong to the same conotoxin superfamily. The conotoxin χ-MrIa was previously shown to belong to the T-superfamily (Mcintosh *et al*, 2000) hence fv1a and χ-AuId are also members of the T-superfamily. (χ-MrIA accession no: GQ981407.1)

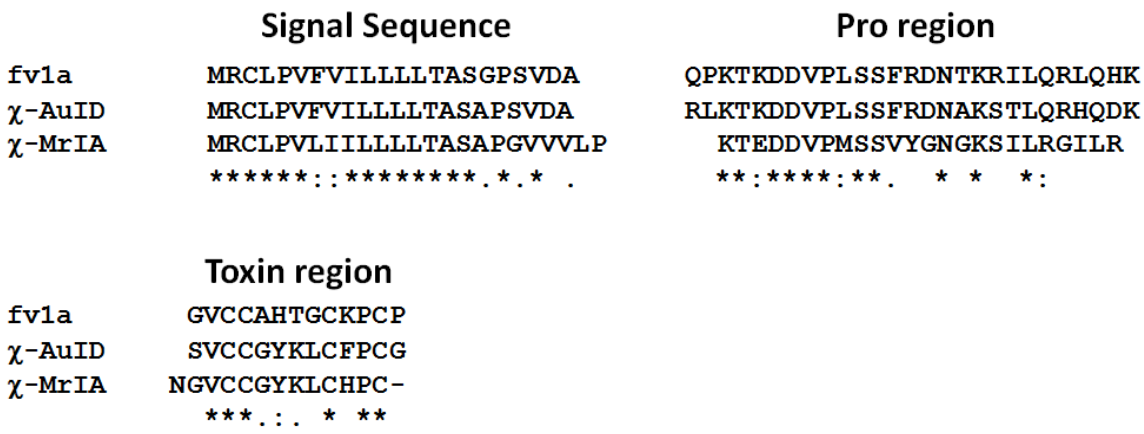
Signal Sequence
Pro region
fv1a MRCLPVFVILLLLTASGPSVDA QPKTKDDVPLSSFRDNTKRILQRLQHK
χ-AuID MRCLPVFVILLLLTASAPSVDA RLKTKDDVPLSSFRDNAKSTLQRHQDK
χ-MrIA MRCLPVLIILLLLTASAPGVVVLP KTEDDVPMSSVYGNGKSILRGILR
Toxin region
fv1a GVCCAHTGCKPCP
χ-AuID SVCCGYKLCFPCG
χ-MrIA NGVCCGYKLCHPC-

Figure 2.7. Comparison of the effects of fv1a and the χ-conotoxins on the response of DRG neurons to depolarization by 25 mM KCl. 25 mM KCl was consecutively applied at 7-min intervals into a culture of dissociated mouse DRG neurons. After the third KCl application, the DRG neurons were incubated with 1.5 μM of the conotoxins. The activity of the conotoxins is seen as the changes in peak height corresponding to fluxes of cytosolic calcium in the KCl pulse immediately following conotoxin incubation. fv1a partially inhibits the cytosolic calcium increase in 13.3 (±2.6)% of the cells whereas the χ-conotoxins cause an amplification of the calcium response of the cells upon KCl depolarization. The percentage of neurons affected by the χ-conotoxins are: χ-AoIC: 4.5 (±0.5)%; χ-AuID: 6.7 (±0.9)%; χ-MrIA: 9.3 (±1.3)%).

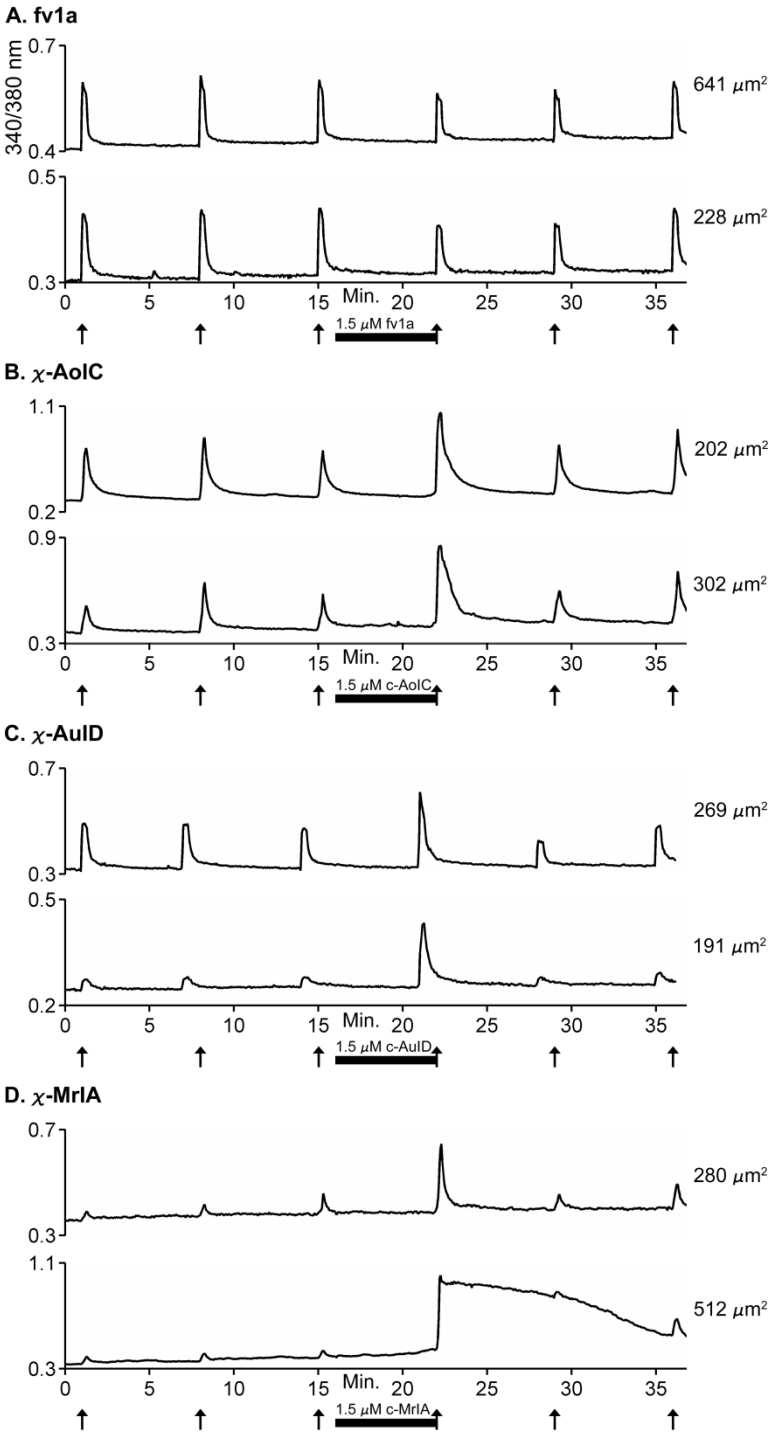
A. fv1a
340/380 nm
0.7
0.4
0.5
0.3
641 μm²
228 μm²
0 5 10 15 Min. 20 25 30 35
1.5 μM fv1a
B. χ-AolC
1.1
0.2
0.9
0.3
202 μm²
302 μm²
0 5 10 15 Min. 20 25 30 35
1.5 μM c-AolC
C. χ-AulD
0.7
0.3
0.5
0.2
269 μm²
191 μm²
0 5 10 15 Min. 20 25 30 35
1.5 μM c-AulD
D. χ-MrlA
0.7
0.3
1.1
0.3
280 μm²
512 μm²
0 5 10 15 Min. 20 25 30 35
1.5 μM c-MrlA

Table 2.1. T-superfamily conotoxins presented and discussed in this paper.

Conotoxin	Sequence	Conus species	Prey	Reference
χ-AuID	**SVCCGYKLCFOC***	*C. aulicus*	mollusk	This work
χ-AoIC	**RCCGYKMCHOC**	*C. araneosus*	mollusk	Gupta et al. 2010; This work
χ-MrIA	**NGVCCGYKLCHOC**	*C. marmoreus*	mollusk	McIntosh et al. 2000; Balaji et al. 2000; Sharpe et al. 2001
fv1a	**GVCCAHTGCKOCP**	*C. furvus*	mollusk	This work

*Indicates C-terminal amidation; O: hydroxyproline; Identical amino acids between the sequences are marked.

References

Adamo SA. 2008. Norepinephrine and octopamine: linking stress and immune function across phyla. Invert Surv J. 5(1): 12 – 19.

Azam L, McIntosh JM. 2009. Alpha-conotoxins as pharamacological probes of nicotonic acetylcholine receptors. Acta Pharmacol Sin. 30(6): 771 – 783.

Balaji RA, Ohtake A, Sato K, Gopalakrishnakone P, Kini RM, Seow KT, Bay BH. 2000. λ-Conotoxins a new family of conotoxins with unique disulfide pattern and protein folding: isolationa and characterization from the venom of *Conus marmoreus*. J Biol Chem. 275(50): 39516 – 39522.

Bönisch H, Brüss M. 2006. The norepinephrine transporter in physiology and disease. Handb Exp Pharmacol. 175: 485-524.

Brust A, Palant E, Croker D, Colless B, Drinkwater R, Patterson B, Schroeder C, Wilson D, Nielsen K, Smith M, Alewood D, Alewood P, Lewis R. 2009. χ-conopeptide pharmacophore development: toward a novel class of norepinephrine transporter inhibitor (Xen2174) for pain. J Med Chem. 52(22): 6991 – 7002.

Buczek O, Bulaj G, Olivera BM. 2005. Conotoxins and the posttranslational modification of secreted gene products. Cell Mol Life Sci. 62(24): 3067-3079.

Bulaj G. 2008. Integrating the doscovery pipeline for novel compounds targeting ion channels. Curr Opin Chem Biol. 12(4): 441 – 447.

Colledge CJ, Hunsperger JP, Imperial JS, Hillyard DR. 1992. Precursor structure of ω-conotoxin GVIA determined from a cDNA clone. Toxicon 30(9): 1111-1116.

Espino SS, Dilanyan T, Imperial JS, Aguilar MB, Teichert RW, Bandyopadhyay P, Olivera BM. 2016. Glycine-rich conotoxins from the *Virgiconus* clade. Toxicon 113: 11 – 17.

Favreau P, Stocklin R. 2009. Marine snail venom: use and trends in receptor and channel pharmacology. Curr Opinion in Pharmacol. 9(5): 594-601.

Galli A, De Felice L, Duke BJ, Moore K, Blakely R. 1995. Sodium-dependent norepinephrine-induced currents in norepinephrine-transporter-transfected HEK 293 cells blocked by cocaine and antidepressants. J Exp Biol. 198: 2197 – 2212.

Green B, Bulaj G, Norton R. 2014. Structure and function of μ-conotoxins, peptide based sodium channel blockers with analgesic activity. Future Med Chem. 6(15): 1677 – 1698.

Gupta K, Kumar M, Balaram P. 2010. Disulfide bond assignment by mass spectrometry of native natural peptides: cysteine pairing in disulfide bonded conotoxins. Anal Chem. 82(19): 8313 – 8319.

Hillyard DR, Olivera BM, Woodward S, Corpuz GO, Gray WR, Ramilo CA, Cruz LJ. 1989. A molluscivorous *Conus* toxin: conserved framework in conotoxins. Biochemistry 289(1): 358 – 361.

Kohn AJ. 1959. The Ecology of *Conus* in Hawaii. Ecol Monographs 29(1): 47-90.

Lacoste A, Malham SK, Cueff A, Jalabert F, Gelebart F, Poulet SA. 2001. Evidence for a form of adrenergic response to stress in the mollusk *Crassostrea gigas*. J Exp Biol. 204(Pt 7): 1247 – 1255.

McIntosh JM, Corpuz GO, Layer RT, Garrett J, Wagstaff JE, Bulaj G, Vyazovkina A, Yoshikami D, Cruz LJ, Olivera BM. 2000. Isolation and characterization of a novel *Conus* peptide with apparent antinociceptive property. J Biol Chem. 275(42): 32391 – 32397.

McIntosh JM, Jones RM. 2001. Cone venom-from accidental stings to deliberate injection. Toxicon 39(10): 1447-1451.

Olivera BM. 2006. Conus peptides: biodiversity-based discovery and exogenomics. J Biol Chem. 281(42): 31173 – 31177.

Olivera BM, Cruz LJ. 2001. Conotoxins, in retrospect. Toxicon 39(1): 7 – 14.

Olivera BM, Teichert RW. 2007. Diversity of the neurotoxic Conus peptides: a model for concerted pharmacological discovery. Mol Interv. 7(5): 251 – 260.

Olivera BM. 1997. E.E. Just Lecture, 1996. Conus venom peptides, receptor and ion channel targets, and drug design: 50 million years of neuropharmacology. Mol Biol Cell 8(11): 2101-2109.

Olivera BM. 2002. *Conus* venom peptides: reflections from the biology of clades and species. Annual Rev Ecol Syst. 33: 25-42.

Olivera BM, Gray WR, Zeikus R, McIntosh JM, Varga J, Rivier J, de Santos V, Cruz LJ. 1985. Peptide neurotoxins from fish-hunting cone snails. Science 230(4732): 1338-1343.

Olivera BM, Rivier J, Clark C, Ramilo CA, Corpuz GP, Abogadie FC, Mena EE, Woodward SR, Hillyard DR, Cruz LJ. 1990. Diversity of *Conus* neuropeptides. Science 249(4966): 257-263.

Platt RJ, Curtice KJ, Twede VD, Watkins M, Gruszczynski P, Bulaj G, Horvath

MP, Olivera BM. 2014. From molecular phylogeny towards differentiating pharmacology for NMDA receptor subtypes. Toxicon 81: 67 – 79.

Puillandre N, Bouchet P, Duda TF Jr, Kauferstein S, Kohn AJ, Olivera BM, Watkins M, Meyer C. 2014. Molecular phylogeny and evolution of the cone snails (Gastropoda, Conoidea). Mol Phylogenet Evol. 78, 290-303.

Robinson SD, Norton RS. 2014. Conotoxin Gene Superfamilies. Mar Drugs. 12(112): 6058-6101.

Röckel D, Korn W, Kohn AJ. 1995. Manual of the Living Conidae. Wiesbaden, Germany: Verlag Christa Hemmen 517p.

Sharpe IA, Gehrmann J, Loughnan ML, Thomas L, Adams DA, Atkins A, Palant E, Craik DJ, Adams DJ, Alewood PF, Lewis RJ. 2001. Two new classes of conopeptides inhibit the a1-adrenoceptor and the noradrenaline transporter. Nat Neurosci. 4(9): 902 – 907.

Sloley BD, Juorio AV, Durden DA. 1990. High performance chromatographic analysis of monoamines and some of their γ-glutamyl conjugates produced by the brain and other tissues of *Helix aspersa* (garstropoda). Cell Mol Neurobiol. 10(2): 175 – 192.

Smith NJ, Hone AJ, Memon T, Bossi S, Smith TE, McIntosh JM, Olivera BM, Teichert RW. 2013. Comparative functional expression of nAChR subtypes in rodent DRG neurons. Front Cell Neurosci. 7: 225.

Teichert RW, Olivera BM, McIntosh JM, Bulaj G, Horvath MP. 2015. The molecular diversity of conoidean venom peptides and their targets: from basic research to therapeutic applications. In: King GF, editor. Venom to drugs: venom as a source for the development of human therapeutics. London: RSC Publishing. p. 163-203.

Teichert RW, Smith NJ, Raghuraman S, Yoshikami D, Light AR, Olivera BM. 2012. Functional profiling of neurons through cellular neuropharmacology. Proc Natl Acad Sci. 109(5): 1388-1395.

Terlau H, Olivera BM. 2004. *Conus* venoms: a rich source of novel ion channel-targeted peptides. Physiol Rev. 84(1): 41-68.

Ul-hasan S, Burgess DM, Gajewiak J, Li Q, Hu H, Yandell M, Olivera BM, Bandyopadhyay P. 2013. Characaterization of the peptidyl glycine α-amidating monooxygenase (PAM) from the venom ducts of the neogastropods *Conus bullatus* and *Conus geographus*. Toxicon 74: 215 – 224.

Walker CS, Steel D, Jacobsen RB, Lirazan MB, Cruz LJ, Hooper D, Shetty R,

DelaCruz RC, Nielsen JS, Zhou LM, Bandyopadhyay P, Craig AG, Olivera BM. 1999. The T-superfamily of conotoxins. J Biol Chem. 274(43): 30664 – 30671.

Woodward SR, Cruz LJ, Olivera BM, Hillyard D. 1990. Constant and Hypervariable Regions in Conotoxin Propeptides. EMBO J. 9(4): 1015-1020.

Zhou J. 2004. Norepinephrine transporter inhibitor and their therapeutic potential. Drugs Future 29(12): 1235-1244.

CHAPTER 3

GLYCINE-RICH CONOTOXINS FROM THE VIRGICONUS CLADE

Toxicon (2016) 113, 11-17. Glycine-rich Conotoxins from the Virgiconus Clade. Espino S.S., Dilanyan T., Imperial J.S., Aguilar M.B., Teichert R.W., Bandyopadhyay P., Olivera B.M.

Toxicon 113 (2016) 11–17

Contents lists available at ScienceDirect

Toxicon

journal homepage: www.elsevier.com/locate/toxicon

Glycine-rich conotoxins from the *Virgiconus* clade

Samuel S. Espino [a], Taleen Dilanyan [a, b], Julita S. Imperial [a, *], Manuel B. Aguilar [c], Russell W. Teichert [a], Pradip Bandyopadhyay [a], Baldomero M. Olivera [a]

[a] Department of Biology, University of Utah, 257 South 1400 East, Salt Lake, UT 84112, USA
[b] Department of Chemistry, Smith College, Northampton, MA 01063, USA
[c] Laboratorio de Neurofarmacología Marina, Departamento de Neurobiología Celular y Molecular, Instituto de Neurobiología, Universidad Nacional Autónoma de México, Campus Juriquilla, Querétaro 76230, México

ARTICLE INFO

Article history:
Received 13 November 2015
Received in revised form
23 January 2016
Accepted 2 February 2016
Available online 4 February 2016

Keywords:
Conotoxins
O1 superfamily
Virgiconus

ABSTRACT

Cone snails in the *Virgiconus* clade prey on marine worms. Here, we identify six related conotoxins in the O1-superfamily from three species in this clade, *Conus virgo*, *Conus terebra* and *Conus kintoki*. One of these peptides, vi6a, was directly purified from the venom of *C. virgo* by following its activity using calcium imaging of dissociated mouse dorsal root ganglion (DRG) neurons. The purified peptide was biochemically characterized, synthesized and tested for activity in mice. Hyperactivity was observed upon both intraperitoneal and intracranial injection of the peptide. The effect of the synthetic peptide on DRG neurons was identical to that of the native peptide. Using the vi6a sequence, five other homologs were identified. These peptides define a glycine-rich subgroup of the O1-superfamily from the *Virgiconus* clade, with biological activity in mice.

Published by Elsevier Ltd.

1. Introduction

Cone snails (family Conidae) are a highly successful group of venomous marine gastropods found in all the tropical oceans. These predatory molluscs can be sorted into three major groups based on their prey preference: fish-hunting (piscivores), mollusc-hunting (molluscivores) and the largest group, worm-hunting (vermivores) (Kohn, 1959; McIntosh and Jones, 2001; Olivera, 1997; Olivera et al., 1990). There are probably ~850 cone snail species (Favreau and Stocklin, 2009; Olivera, 2002; Röckel et al., 1995) and all of them possess venom, which contains a complex array of small peptidic molecules called conotoxins/conopeptides (Olivera et al., 1985, 1990; Teichert et al., 2015; Terlau and Olivera, 2004) that the animal uses for diverse biotic interactions, including prey capture.

The conotoxins are gene products that are initially translated as a precursor (Buczek et al., 2005; Olivera, 1997), which can be divided into three regions: the signal sequence at the N-terminus, the pro region and the mature toxin region at the C-terminus (Colledge et al., 1992; Robinson and Norton, 2014). All conotoxins that share a highly conserved signal sequence can be grouped into a conotoxin gene superfamily; members of a gene superfamily also share a distinct pattern of cysteine residues in their amino acid sequence (Terlau and Olivera, 2004; Woodward et al., 1990). Each conotoxin superfamily can be further subdivided into pharmacological families (Terlau and Olivera, 2004). For example, the O1-conotoxin superfamily comprises the ω-conotoxins, which target voltage-gated calcium channels (Hillyard et al., 1992; Olivera et al., 1985; Zhangsun et al., 2006), the κ-conotoxins, which target voltage-gated potassium channels (Shon et al., 1998; Terlau et al., 1996) and the δ- and the μO-conotoxin families, which target voltage-gated sodium channels at different sites (Leipold et al., 2005; McIntosh et al., 1995; Shon et al., 1995; Terlau et al., 1996; Wilson et al., 2015).

Many members of the O1-conotoxin super family that were shown to be biologically active in vertebrates were purified from the venom of fish-hunting cone snails (Terlau and Olivera, 2004). This is not surprising since fish-hunting cone snails evolved their highly expressed conotoxins to potently target their fish prey. However, worm-hunting and mollusc-hunting cone snails do express conotoxins that target specific molecules in vertebrates. We focused this study on cone snails that belong to the vermivorous *Virgiconus* clade. There are at least nine species, all from the Indo-Pacific region, in this clade (Puillandre et al., 2014). Three species from this clade namely: *Conus virgo*, *Conus terebra* and *Conus kintoki*

* Corresponding author..
E-mail addresses: imperial@biology.utah.edu, jimperial98@gmail.com (J.S. Imperial).

http://dx.doi.org/10.1016/j.toxicon.2016.02.001
0041-0101/Published by Elsevier Ltd.

(shown in Fig. 1) were analyzed; *C. virgo* and *C. terebra* are shallow-water species, while *C. kintoki* is only collected well offshore, at depths between 50 and 200 m.

In this paper, six homologous O1-superfamily conotoxins from three cone snail species were identified. One was purified from the venom of *C. virgo* and we propose to name this conopeptide vi6a. This peptide is active on a subset of mouse dorsal root ganglion (DRG) neurons and elicits a behavioral phenotype in mice upon both intraperitoneal (IP) and intracranial (IC) injection. Homologous peptides were identified from *C. terebra* and *C. kintoki*, as well as two additional peptides from *C. virgo*. These conotoxins are unusually glycine-rich, and define a novel subgroup within the O1-superfamily.

2. Materials and methods

2.1. Extraction of crude venom

Lyophilized *C. virgo* venom was homogenized in 10 mL of 35% (v/v) CH_3CN – 0.1% (v/v) trifluoroacetic acid (TFA) using a glass-PTFE tissue grinder for 5 cycles at 1500 rpm. The homogenate was centrifuged in a Beckmann F0650 rotor at 37,000 × g for 15 min at 5 °C and the supernatant containing the crude venom extract was collected.

2.2. Venom fractionation

The crude venom extract was fractionated by Reversed-Phase High Performance Liquid Chromatography (RP-HPLC) using a Vydac C18 preparative column (218TP101522). Elution was done at a flow rate of 7 mL/min and using a two solvent system: Solvent A (0.1% TFA) and Solvent B (90% v/v CH_3CN, 0.1% v/v TFA). The elution gradient used was made up of the following steps: 2%–55% Solvent B for 53 min, 55%–65% for 5 min and 65%–100% for 5 min. Solvent B was maintained at 100% for 1 min and then brought down to 10% within 3 min. The subfractionation of the active fraction 15 was done by analytical RP-HPLC using a C18 Vydac monomeric column (238EV54) and using the following gradient: 5%–10% Solvent B for 5 min, 10%–25% Solvent B for 45 min. The absorbance was monitored at 220 and 280 nm.

2.3. Reduction and alkylation of the purified peptides

The bioactive peptide from *C. virgo* was reduced using dithiothreitol (DTT) and was alkylated using 4-vinylpyridine (4-VP). The pH of the solution containing the peptide was buffered to pH 8 using 0.5 M Tris base. The peptide was reduced with 10 mM DTT at 65 °C for 30 min. A 0.8 μL volume of 4-VP was added to the solution containing the reduced peptide. The alkylation of the reduced peptide was performed in the dark at room temperature for 30 min. The reduced and alkylated peptide was purified from the reaction by analytical RP-HPLC using a gradient similar to that previously described for the analytical HPLC purification of fraction 15.

2.4. Peptide sequencing

The sample was dissolved in 30 μL of solvent B (90% v/v CH_3CN, 0.1% v/v TFA). Thirty microliters of the solution were applied to a glass fiber Micro TFA Filter (401111, Applied Biosystems, Foster City, CA) previously treated with 15 μL of Biobrene Plus (400385, Applied Biosystems), dried with Argon, and then sequenced for 34 cycles in a Procise 491 Protein Sequencing System (Applied Biosystems) employing the Pulsed-liquid method.

2.5. Identification and sequencing of O-superfamily conotoxin clones from Conus virgo, Conus terebra and Conus kintoki

RNA from the venom duct dissected from a single specimen each of *C. virgo*, *C. terebra* and *C. kintoki* was isolated using TRIzol® reagent (Invitrogen, Grand Island, NY) following the manufacturer's recommended protocol. cDNA was synthesized from total RNA using the SMART PCR cDNA synthesis kit (Clontech, Mountain View, CA) according to the manufacturer's protocols. The first strand cDNA was used as a template for the PCR amplification of O1-superfamily conotoxin genes using the primers Osup+ (5′-ATGAAACTGACGTGYGT-3′) and Osup- (5′- TACGTYCTCTGAATY-CACCAGAG-3′). These primers were designed based on the conserved region of the O1-superfamily precursor. The PCR products were gel-purified using PCR product purification kit (Qiagen, Valencia, CA) and ligated into pGEM®-T Easy vector (Promega, Madison, WI) following the manufacturer's standard protocol. The products from these reactions were transformed into competent *E. coli* DH10β cells (New England Biolabs, Inc, Ipswich, MA). The colonies were screened by PCR using the Osup+ and the Osup- primers. Positive clones were sequenced using the T7 and SP6 promoter primer sequences (Promega, Madison, WI).

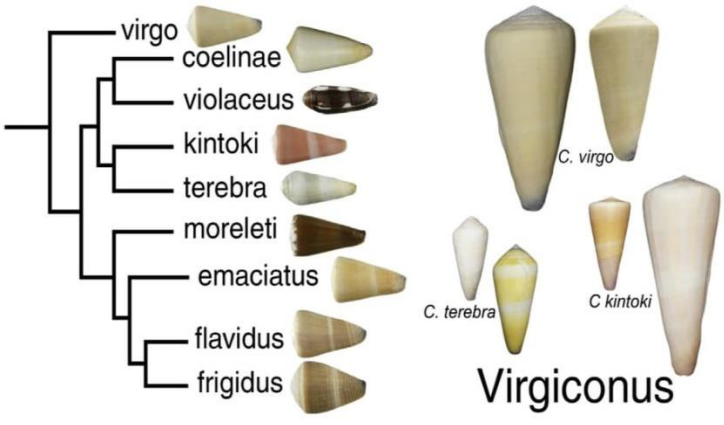

Fig. 1. Phylogenetic relationships in the Virgiconus clade. The snails where the conotoxins reported in this paper were found are shown on the right. The largest specimen in this figure is C. kintoki, which measures 111 mm.

2.6. Solid phase peptide synthesis of vi6a

Linear vi6a was synthesized at a 50-μmol scale using an AAPPTec Apex 396 synthesizer (AAPPTec LLC, Louisville, KY) applying standard solid-phase Fmoc (9-fluorenylmethyloxycarbonyl) protocols. Fmoc-protected amino acids, were purchased from AAPPTec. N-α-Fmoc-O-t-butyl-L-trans-4-hydroxyproline (Hyp) was purchased from EMD Millipore (Darmstadt, Germany). The peptides were assembled on pre-loaded Fmoc-L-Leu-Wang resin (substitution: 0.33 mmol g^{-1}; Peptides International Inc., Louisville, KY), Fmoc-Gln(Trt)-Wang resin (substitution: 0.57 mmol g^{-1}, Nova-Biochem, EMD Millipore), Fmoc-Ser(tBu)-Wang resin (substitution: 0.53 mmol g^{-1}; Peptides International, Louisville, KY). Side-chain protection for each amino acid was: Arg, 2,2,4,6,7-pentamethyldihydrobenzofuran-5-sulfonyl (Pbf); Asp and Glu, O-*tert*-butyl (OtBu); Lys, *tert*-butyloxycarbonyl (Boc) Hyp, Thr and Tyr, *tert*-butyl (tBu); and Gln and Cys, trytl (Trt). Coupling of each amino acid was achieved using 1 equivalent of 0.4 M benzotriazol-1-yl-oxytripyrrolidinophosphonium hexafluorophosphate (PyBOP) and 2 equivalents of 2 M *N*,*N*-diisopropylethyl amine (DIPEA) in *N*-methyl-2-pyrrolidone (NMP). Standard amino acids were used in ten-fold excess (60-min coupling), with the exception of Arg and Hyp, which were used in five-fold excess (90-min coupling). Fmoc-protecting groups were removed by a 20-min treatment with 20% (v/v) piperidine in dimethylformamide (DMF).

2.7. Oxidative folding of vi6a

The linear vi6a was resuspended in 0.5 mL of 0.01% TFA solution and added to a solution containing: 2.5 mL of 0.2 M Tris•HCl (pH 7.5) + 0.2 mM EDTA, 0.5 mL of 1:1 mixture of 20 mM reduced (GSH) and oxidized (GSSG) glutathione and 1.5 mL of water. The final peptide concentration in the folding mixture was 20 μM. The linear vi6a was folded for 2 h and the reaction was quenched with 8% (v/v) formic acid. The reaction mixture was separated by RP-HPLC using a Vydac semi-preparative C_{18} column and employing a linear gradient from 5% to 40% Solvent B for 35 min at a flow rate of 4 mL/min. The eluent was monitored by absorbance at 220 nm and at 280 nm. The purity of the folded peptides was assessed by analytical RP-HPLC using the gradient described above, with a flow rate 1 mL/min. The concentration of the folded peptide was determined by UV/Vis spectrophotometry at 280 nm and using an extinction coefficient (ε) of 1420 L mol^{-1} cm^{-1}. The mass was determined by matrix-assisted laser desorption ionization mass spectrometry (MALDI-MS).

2.8. Co-elution experiment of the native and synthetic vi6a

The co-elution experiments were done using analytical RP-HPLC. One nmol of each of the native and synthetic vi6a was separately injected into the analytical C_{18} column and eluted using a gradient of 5%–40% Solvent B for 35 min. A mixture containing 1 nmol of each of the native and synthetic vi6a was also analyzed on the same column using the same gradient.

2.9. Calcium imaging assay

Experimental protocols involving live animals were approved by the Institutional Animal Care and Use Committee (IACUC) of the University of Utah. Preparation of the cell cultures from dorsal root ganglia (DRG) and calcium imaging experiments were done as described previously (Smith et al., 2013; Teichert et al., 2012). Briefly, lumbar DRG neurons from wild type C57BL/6 mice were dissociated, pooled and cultured overnight for calcium imaging experiments. Cells were loaded with Fura-2-AM dye 1 h before the experiment. During the experiment, the dye inside the cells was excited alternately with 340 nm and 380 nm light. The ratio of the emission at 510 nm from both excitations was measured. The ratio of the fluorescence intensity is a measure of the increase in cytosolic calcium $[Ca^{2+}]_i$ resulting from the depolarization caused by the external application of a high concentration of potassium ions, $[K^+]_o$. For the purification of the bioactive component from *C. virgo* venom, a solution containing 20 μM $[K^+]_o$ and 20 μM veratridine was used to depolarize the DRG neurons. Veratridine prolongs the activation of voltage-gated sodium channels and facilitates the discovery of venom components that may block sodium channels, in addition to those that may act on potassium or calcium channels. This solution was applied every 7 min. After the third depolarizing pulse, crude *C. virgo* venom extract or HPLC fractions were incubated with the cells for 7 min. The fourth depolarizing pulse was applied to identify the effect of the applied venom or fractions on the DRG neurons. Succeeding depolarizing pulses were done to determine the reversibility of the observed effects. A similar protocol was followed for the assessment of the activity of the synthetic vi6a; however, 30 mM $[K^+]_o$ was used as the depolarizing stimulus and the experiment was performed without veratridine.

2.10. Mouse bioassay

Swiss Webster mice (17 – 19 days; 7 – 10 g) were injected intracranially (IC) with the peptide in 10 μL normal saline solution (NSS). Mice were observed for aberrant behavior for 3 h. The systemic effect of vi6a was determined by the intraperitoneal (IP) injection of the peptide into 17 – 19 day old mice. Appropriate concentrations of the peptide were dissolved in 50 μL NSS and injected IP into mice. The mice were then observed for 3 h. The use of Swiss Webster mice followed protocols that conform to the National Institutes of Health Guide for the Care and Use of Laboratory Animals and approved by the University of Utah Institutional Animal Care and Use Committee.

3. Results

3.1. Purification of a biologically active conotoxin from the venom of Conus virgo

Venom extracted from *Conus virgo* venom glands was assayed based on its activity in the calcium imaging of dissociated mouse dorsal root ganglion (DRG) neurons. This assay measures the changes in cytosolic calcium $[Ca^{2+}]_i$ in response to a stimulus. In this paper, the effect of venom or conotoxins on the changes in $[Ca^{2+}]_i$ resulting from depolarization by the application of high extracelluar potassium $[K^+]_o$ is measured. Diverse activities were observed when the venom was subjected to this assay. In some cells, the application of the crude extract of the venom from *C. virgo* resulted in the inhibition of the increase in $[Ca^{2+}]_i$ resulting from a depolarizing pulse of 20 mM $[K^+]_o$ with 20 μM veratridine. In other cells, the depolarizing pulse following venom application resulted in an increase in $[Ca^{2+}]_i$. Other cells showed a direct response (i.e. a perturbation of the baseline upon venom application). The component responsible for the inhibition of the increase in $[Ca^{2+}]_i$ was further purified from the venom using reversed-phase high performance liquid chromatography (RP-HPLC) (Fig 2).

Individual HPLC fractions were tested and the inhibitory activity was found in fraction 15. Subfractionation of this fraction resulted in a single major component (Fig. 2B) that retained the inhibitory activity. The bioactive, major fraction in Fig. 2B was shown to be homogeneous by linear mode MALDI-MS.

3.2. Biochemical characterization of the inhibitory compound from C. virgo venom

Analysis of the purified fraction (Fig. 2B) by electrospray ionization mass spectrometry (ESI-MS) revealed a homogeneous solution containing a component with a mass of 3114.15 Da. When the component that exhibited the inhibitory activity was reduced and alkylated (see Methods), MALDI-MS in the linear mode yielded a mass of 3754.16 Da. The difference of 640.01 Da between the native compound and the reduced/alkylated compound suggested the presence of 6 cysteine residues that were alkylated by 6 molecules of 4-vinylpyridine (MW 105 Da).

N-terminal sequencing of the active component revealed the peptide sequence to be: D**C**GGQGEG**C**YTQO**C-C**OGLR**C**RGGGTGGGV**C**QL. This peptide is 32 amino acids long and contains 6 cysteine residues consistent with the number of cysteine residues identified from the comparison of the masses of the native and reduced/alkylated peptides. The arrangement of the cysteine

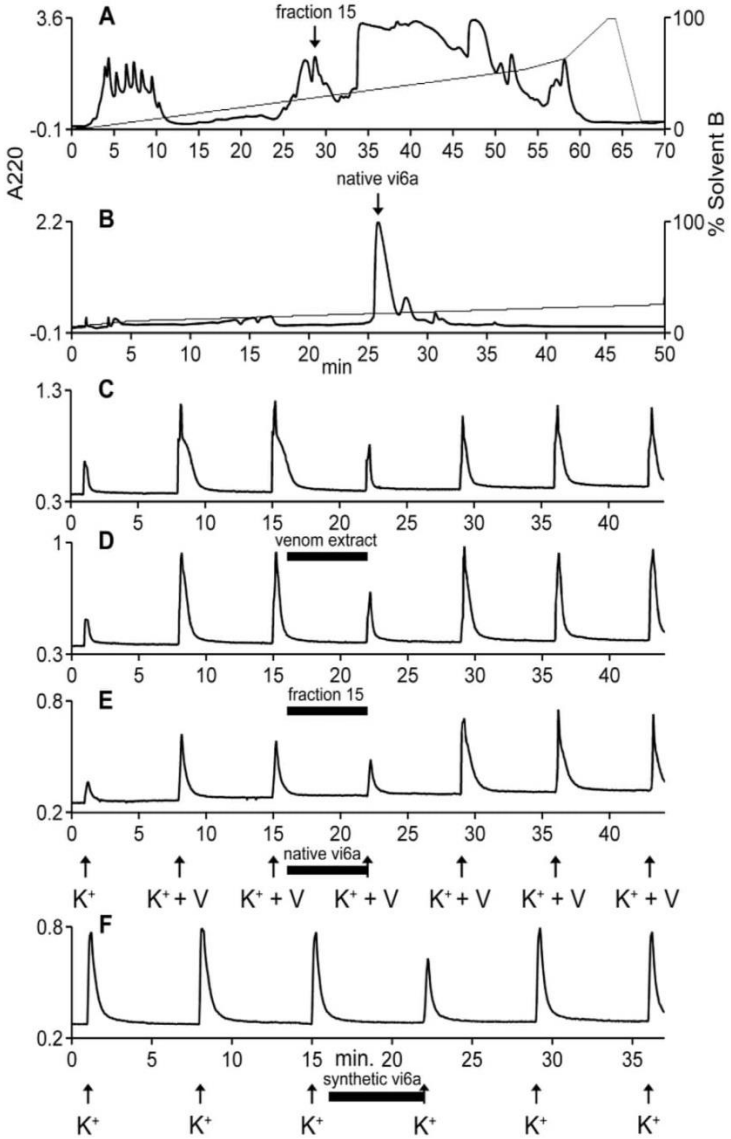

Fig. 2. Bioactivity-guided purification of the inhibitory component from *C. virgo* venom. HPLC fractions of the *C. virgo* venom extract was screened for the activity to inhibit the increase in intracellular calcium upon depolarization with 20 mM $[K^+]_o$ and 20 μM veratridine. Fraction 15, marked by the arrow in A, showed the inhibitory activity. Further subfractionation of the inhibitory fraction yielded a single major active component (native vi6a) indicated by the arrow in B. MALDI-MS in the linear mode of the major peak in B revealed the fraction to contain only vi6a. C – E are the calcium imaging traces of the DRG neurons showing the inhibitory activity. The Y-axis of each graph is the 340/380 nm ratio described in Methods. The arrows represent the 15-s application of 20 mM $[K^+]o$ and 20 μM veratridine, and the horizontal bars indicate the time when each sample was present in the bath solution. Panel C shows the inhibitory activity of the crude venom extract; panel D shows the inhibitory activity of fraction 15 and panel E shows the inhibitory activity of the native vi6a. Panel F shows the inhibitory activity of the synthetic peptide. In panel F, the arrows indicate the 15 s application of 30 mM $[K^+]_o$. In panels C–F, the horizontal bar indicates the time when each sample was present in the bath solution.

Fig. 3. Alignment of conotoxin sequences predicted from clones obtained from *C. virgo* (Vi), *C. terebra* (Tr) and *C. kintoki* (Kt). Vi6.1 is the precursor sequence that codes for vi6a, the peptide purified from the venom of *C. virgo*. These sequences display a high degree of similarity indicating that they are members of the same gene family. The amino acids that diverge from Vi6.1 are highlighted and conserved amino acids are identified by an asterisk. Vi6.1 is identical to the Conoserver Vi6.1 protein.

residues of this peptide suggests that it belongs to the O1-conotoxin superfamily. The peptide contains two proline residues that are post translationally modified to hydroxyproline. One striking feature of this peptide sequence is the abundance of glycine residues. Of the 26 non-cysteine residues, 11 are glycine residues.

The peptide sequence assignment was verified by the chemical synthesis of the peptide with the above sequence. Analysis of the folding reaction revealed the formation of a single major component after 2 h. This major component was purified to >99% purity from the folding reaction using RP-HPLC. MALDI-MS in the reflector mode revealed a mass of 3114.10 Da, which matches the mass of the native peptide previously determined using ESI-MS. Co-elution was carried out to verify whether the synthetic and the native peptides are structurally identical (Fig. S1). Separate injections of 1 nmol each of the synthetic and native peptides in an analytical HPLC column at a gradient of 5%–40% B90 for 35 min revealed a similar retention time of ~16 min for both peptides. A solution containing 1 nmol each of the native and the synthetic peptides was analyzed using the same HPLC gradient; a single peak eluted at ~16 min indicating the co-elution of the native and synthetic peptides (Fig. S1). These experiments validated the sequence assignment and suggest that the folding reaction formed a major component whose disulfide connectivity matches that of the native peptide. We propose to call this peptide vi6a.

3.3. Sequencing of clones from C. virgo, C. terebra, and C. kintoki

Conotoxins are initially translated as larger prepropeptide precursors. The precursor sequence of vi6a was determined using PCR primers designed to hybridize to the conserved region of the O1-superfamily precursor. We also screened cDNA's extracted from *C. terebra,* and *C. kintoki* for the presence of O1-superfamily conotoxins to determine whether these snails express conotoxins with sequences similar to vi6a (these cone snail species, like *C. virgo*, are members of the *Virgiconus* clade). The peptides predicted from clones Vi6.1, Vi6.2 and Vi6.4 from *C. virgo* are shown in Figs. 3 and 4; the predicted toxin from Vi6.1 exactly matches the sequence of vi6a.

Thus, the Vi6.1 clone encodes the precursor sequence of vi6a. The screening of the *C. terebra* cDNA yielded two clones: Tr6.2 and Tr6.3 (Figs. 3 and 4) whose predicted toxins are homologous to vi6a. The clone Kt6.1 (Figs. 3 and 4) from *C. kintoki* also codes for a homologous peptide. These sequences are compared in Figs. 3 and 4. The high degree of similarity in the signal sequences of these precursors indicates that these conotoxins belong to the O1 – superfamily.

3.4. Biological activity of vi6a

The biological activity of the synthetic vi6a was assessed using the calcium imaging assay. In these experiments, DRG neurons were depolarized by external application of 30 mM $[K^+]_o$ once every 7 min. After the third depolarization, 1 μM vi6a was applied and allowed to incubate with the cells for 6 min. Cellular response was assessed upon the fourth application of 30 mM $[K^+]_o$ immediately following the 1 μM vi6a incubation. Results from 3 experiments using DRG neurons prepared from 3 different mice showed that the synthetic vi6a exhibited the inhibitory activity in 76 ± 10% of the cells. The inhibitory effect of vi6a is observed in small, medium and large diameter DRG neurons. A sample calcium imaging trace showing the inhibitory activity of the synthetic vi6a is shown in Fig 2F.

The peptide, vi6a, was also tested for its *in vivo* effects upon injection into mice. An intracranial (IC) injection of the peptide dissolved in 10 μL normal saline solution (NSS) and injected into 17 – 19 day old mice elicited the behavioral phenotypes shown in Table 1. Mice injected with 0.4 mg/kg vi6a exhibited a hyperactive phenotype manifested by the injected animal (n = 3) continuously running around the cage. Increasing the amount of vi6a to 2.0 mg/kg resulted in the typical hyperactive phenotype; animals would climb the cage, jump and run around.

The systemic effects of vi6a on mice were determined by the intraperitoneal (IP) injection of vi6a (Table 1). Mice between 17 and 19 days old were used for the experiment. Varying amounts of vi6a were dissolved in 50 μL normal saline solution (NSS). IP injection of vi6a (0.7 mg/kg) resulted in the same hyperactive phenotype observed when the peptide was injected IC into mice. Increasing the dose of vi6a to 6.0 mg/kg also elicited the same hyperactive phenotype, which lasted longer than the effects of the lower doses of vi6a.

4. Discussion

In this paper, a subset of conotoxins expressed by cone snails belonging to the worm-hunting *Virgiconus* clade has been identified. There are at least nine known cone snail species belonging to this clade and these snails are widely distributed across the tropical Indo-Pacific ranging from inter-tidal regions to deep waters. Venoms of species in this clade have not been well characterized. We purified a peptide from *C. virgo* based on its biological activity in the calcium imaging of dissociated mouse DRG neurons. Using molecular biology techniques, five other related conotoxins from the *Virgiconus* clade were identified. It seems likely that all species

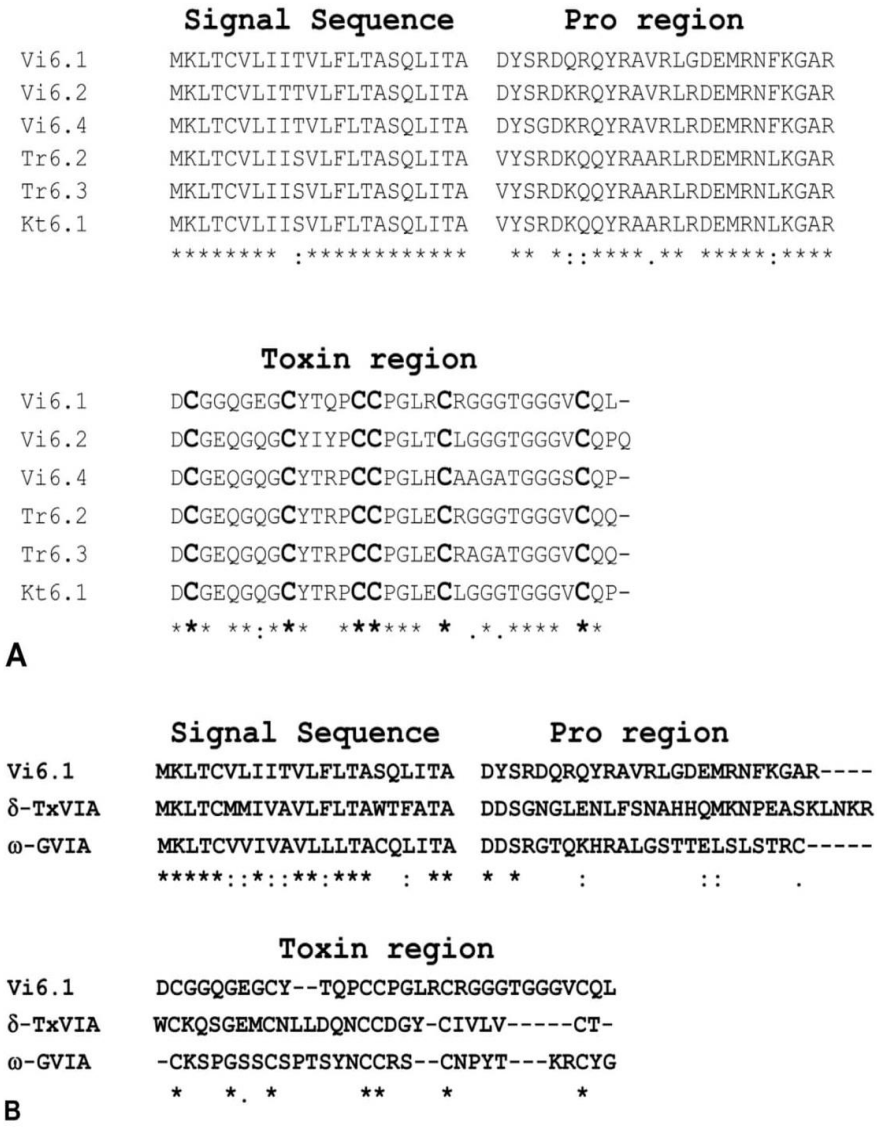

Fig. 4. A. Alignment of the precursor sequence of vi6a (Vi6.1) with the precursor sequences of conotoxins identified from *C. virgo*, *C. terebra* and *C. kintoki*. The amino acid sequences of these precursors are highly conserved indicating that these conotoxins belong to the same gene family. The conserved amino acids are marked by an asterisk. B. Alignment of the precursor sequence of vi6a (Vi6.1) with the precursor sequence of known O1-superfamily conotoxins from the delta conotoxin family (δ-TxVIA) and the omega conotoxin family (ω-GVIA). These precursor sequences have a very high degree of similarity in the signal sequence and a conserved pattern of cysteine residues in the conotoxin region indicating that they belong to the same superfamily. The signal sequence of Vi6.1 is more similar to the signal sequence of ω-GVIA(ω-GVIA accession number: M84612.1; δ-TxVIA accession number: AF193261.1).

in the *Virgiconus* clade express related peptides.

We note that *Conus virgo* has three peptides in this group that have between 8 and 9 amino acid substitutions, and are presumably functionally divergent. However, across species, three sequences (Vi6.1, Tr6.2 and Kt6.1) are much more similar (differing by 2–6 amino acids) — these are presumably interspecific variants of peptides with the same molecular target.

The amino acid sequence of vi6a is identical to the amino acid sequence of the predicted toxin contained in precursor virgo 1, previously cloned from the same species by Kauferstein et al. (2005). Since post-translational modifications of amino acids cannot be predicted from the clone, the purification of vi6a from the *C. virgo* venom and the subsequent biochemical characterization of the peptide (reported in this paper) allowed for the identification of the post translational modification of the prolines at positions 13 and 16 into hydroxyproline. The clone Vi6.1, which we identified from the *C. virgo* cDNA, is identical to the clone virgo 1.

The pattern of cysteine residues in vi6a matches the cysteine pattern of peptides in the O-conotoxins (i.e. the O1, O2 and O3 superfamilies) (Kaas et al., 2008, 2012; Puillandre et al., 2012). A comparison of the signal sequences to known O1-superfamily conotoxins such as δ-TxVIA and ω-GVIA (Fig 4B) reveals that there is a high degree of amino acid conservation. An analysis by means of the ConoPrec tool of the ConoServer database (Kaas et al., 2008, 2012) suggested that all six precursor sequences are most

Table 1
Biological activity of vi6a injected IC and IP into 17 − 19 day old mice.

Assay	Dose injected	Effect	Duration
IC injection	0.4 mg/kg	hyperactivity[a]	not determined
	2.0 mg/kg	hyperactivity[a]	not determined
IP injection	0.7 mg/kg	hyperactivity[a]	20 − 40 min
	2.0 mg/kg	hyperactivity[a]	40 − 60 min
	6.0 mg/kg	hyperactivity[a]	>2 h

These assays used three mice for each dose tested.
[a] Hyperactivity symptoms include continuous running, jumping and climbing in cages.

similar (>92% identity) to signal sequences of the O1-superfamily. We conclude that vi6a and other related peptides in the *Virgiconus* clade are members of the O1-superfamily, and the peptides we have defined in this study comprise a distinctive glycine-rich subgroup within the O1 superfamily.

One of the peptides that we identified, vi6a, has been chemically synthesized and more extensively characterized. As expected from its activity on mouse DRG neurons, vi6a, is active in mammalian systems. The activity of the native peptide observed on dorsal root ganglion cells (see Fig 2), was a decrease in the influx of calcium upon depolarization using high $[K^+]_o$, an activity that was also exhibited by the chemically synthesized peptide. Surprisingly however, when the peptide was injected into mice, both IC and IP, it elicited hyperactivity in the injected animals. The juxtaposition of the *in* vivo excitatory symptomatology and the inhibitory effect on Ca^{2+} influx in response to high $[K^+]_o$ in DRG neurons was unexpected and difficult to explain; the excitatory phenotype elicited upon IP injection into mice is particularly noteworthy. Thus, vi6a has a unique profile of biological activity in mice, the molecular basis of which is currently being investigated.

Acknowledgments

This work was supported by a grant from the National Institute of General Medical Science, GM 48677. We thank Joanna Gajewiak for synthesizing the linear vi6a, William Low for MS analyses, Terry Merritt and Roxanne Ghaffarian for helping prepare the manuscript and My Huynh for assembling some of the figures.

Appendix A. Supplementary data

Supplementary data related to this article can be found at http://dx.doi.org/10.1016/j.toxicon.2016.02.001.

Transparency document

Transparency document related to this article can be found online at http://dx.doi.org/10.1016/j.toxicon.2016.02.001.

Ethical statement

The authors of this paper would like to confirm that they have read and accept the Elsevier ethics statement regarding ethical standards in conducting research, writing an article and authorship.

Conflict of interest

The authors declare that there are no conflicts of interest.

References

Buczek, O., Bulaj, G., Olivera, B.M., 2005. Conotoxins and the posttranslational modification of secreted gene products. Cell Mol. Life Sci. 62, 3067–3079.
Colledge, C.J., Hunsperger, J.P., Imperial, J.S., Hillyard, D.R., 1992. Precursor structure of ω-conotoxin GVIA determined from a cDNA clone. Toxicon 30, 1111–1116.
Favreau, P., Stocklin, R., 2009. Marine snail venom: use and trends in receptor and channel pharmacology. Curr Opin. Pharmacol. 594–601.
Hillyard, D.R., Monje, V.D., Mintz, I.M., Bean, B.P., Nadasdi, L., Ramachandran, J., Miljanich, G., Azimi-Zoonooz, A., McIntosh, J.M., Cruz, L.J., Imperial, J.S., Olivera, B.M., 1992. A new *Conus* peptide ligand for mammalian presynaptic Ca^{2+} channels. Neuron 9, 69–77.
Kaas, Q., Westermann, J.C., Halai, R., Wang, C.K., Craik, D.J., 2008. ConoServer, a database for conopeptide sequences and structures. Bioinformatics 24, 445–446.
Kaas, Q., Yu, R., Jin, A.H., Dutertre, S., Craik, D.J., 2012. ConoServer: updated content, knowledge, and discovery tools in the conopeptide database. Nucleic Acids Res. 40, D325–D330.
Kauferstein, S., Melaun, C., Mebs, D., 2005. Direct cDNA cloning of novel conopeptide precursors of the O-superfamily. Peptides 26, 361–367.
Kohn, A.J., 1959. The Ecology of *Conus* in Hawaii. Ecol. Monogr. 29, 47–90.
Leipold, E., Hansel, A., Olivera, B.M., Terlau, H., Heinemann, S.H., 2005. Molecular interaction of delta-conotoxins with voltage-gated sodium channels. FEBS Lett. 579, 3881–3884.
McIntosh, J.M., Hasson, A., Spira, M.E., Gray, W.R., Li, W., Marsh, M., Hillyard, D.R., Olivera, B.M., 1995. A new family of conotoxins that blocks voltage-gated sodium channels. J. Biol. Chem. 270, 16796–16802.
McIntosh, J.M., Jones, R.M., 2001. Cone venom–from accidental stings to deliberate injection. Toxicon 39, 1447–1451.
Olivera, B.M., 1997. E.E. Just Lecture, 1996. Conus venom peptides, receptor and ion channel targets, and drug design: 50 million years of neuropharmacology. Mol. Biol. cell 8, 2101–2109.
Olivera, B.M., 2002. *Conus* venom peptides: reflections from the biology of clades and species. Annual Review of Ecology. Evol. Syst. 33, 25–42.
Olivera, B.M., Gray, W.R., Zeikus, R., McIntosh, J.M., Varga, J., Rivier, J., de Santos, V., Cruz, L.J., 1985. Peptide neurotoxins from fish-hunting cone snails. Science 230, 1338–1343.
Olivera, B.M., Rivier, J., Clark, C., Ramilo, C.A., Corpuz, G.P., Abogadie, F.C., Mena, E.E., Woodward, S.R., Hillyard, D.R., Cruz, L.J., 1990. Diversity of *Conus* neuropeptides. Science 249, 257–263.
Puillandre, N., Bouchet, P., Duda, T.F., Kauferstein, S., Kohn, A.J., Olivera, B.M., Watkins, M., Meyer, C., 2014. Molecular phylogeny and evolution of the cone snails (Gastropoda, Conoidea). Mol. Phylogenet Evol. 78, 290–303.
Puillandre, N., Koua, D., Favreau, P., Olivera, B.M., Stocklin, R., 2012. Molecular phylogeny, classification and evolution of conopeptides. J. Mol. Evol. 74, 297–309.
Robinson, S.D., Norton, R.S., 2014. Conotoxin gene superfamilies. Mar. Drugs 6058–6101.
Röckel, D., Korn, W., Kohn, A.J., 1995. Manual of the Living Conidae. Verlag Christa Hemmen. Germany, Wiesbaden.
Shon, K., Grilley, M.M., Marsh, M., Yoshikami, D., Hall, A.R., Kurz, B., Gray, W.R., Imperial, J.S., Hillyard, D.R., Olivera, B.M., 1995. Purification, characterization and cloning of the lockjaw peptide from *Conus purpurascens* venom. Biochemistry 34, 4913–4918.
Shon, K., Stocker, M., Terlau, H., Stühmer, W., Jacobsen, R., Walker, C., Grilley, M., Watkins, M., Hillyard, D.R., Gray, W.R., Olivera, B.M., 1998. k-Conotoxin PVIIA: a peptide inhibiting the *Shaker* κ^+ channel. J. Biol. Chem. 273, 33–38.
Smith, N.J., Hone, A.J., Memon, T., Bossi, S., Smith, T.E., McIntosh, J.M., Olivera, B.M., Teichert, R.W., 2013. Comparative functional expression of nAChR subtypes in rodent DRG neurons. Front. Cell Neurosci. 225.
Teichert, R.W., Olivera, B.M., McIntosh, J.M., Bulaj, G., Horvath, M.P., 2015. The molecular diversity of conoidean venom peptides and their targets: from Basic research to Therapeutic applications. In: King, G.F. (Ed.), Venom to Drugs: Venom as a Source for the Development of Human Therapeutics. RSC Publishing, London, pp. 163–203.
Teichert, R.W., Smith, N.J., Raghuraman, S., Yoshikami, D., Light, A.R., Olivera, B.M., 2012. Functional profiling of neurons through cellular neuropharmacology. Proc. Natl. Acad. Sci. U. S. A. 109, 1388–1395.
Terlau, H., Olivera, B.M., 2004. *Conus* venoms: a rich source of novel ion channel-targeted peptides. Physiol. Rev. 84, 41–68.
Terlau, H., Shon, K., Grilley, M., Stocker, M., Stühmer, W., Olivera, B.M., 1996. Strategy for rapid immobilization of prey by a fish-hunting cone snail. Nature 381, 148–151.
Wilson, M.J., Zhang, M.-M., Gajewiak, J., Azam, L., Rivier, J., Olivera, B., Yoshikami, D., 2015. A- and β-subunit composition of voltage-gated sodium channels investigated with μ-conotoxins and the recently discovered μOβ-conotoxin GVIIJ. J. Neurophysiol. 2289–2301.
Woodward, S.R., Cruz, L.J., Olivera, B.M., Hillyard, D.R., 1990. Constant and hypervariable regions in conotoxin propeptides. Embo J. 9, 1015–1020.
Zhangsun, D., Luo, S., Wu, Y., Zhu, X., Hu, Y., Xie, L., 2006. Novel O-superfamily conotoxins identified by cDNA cloning from three vermivorous conus species. Chem. Biol. Drug Des. 68, 256–265.

CHAPTER 4

FUNCTIONAL CHARACTERIZATION OF PRURICEPTORS IN THE MOUSE DORSAL ROOT GANGLION (DRG)

Abstract

Itch is defined as an unpleasant sensation that causes the reflex to scratch. The sensation of itch known as pruriception is detected by neurons whose cell bodies are found in the dorsal root ganglion (DRG). Itch is classified as either histamine-dependent or histamine-independent. Here we showed three classes of neurons from the mouse dorsal root ganglion (DRG) that respond to histamine and chloroquine. Class A (His+) neurons respond to histamine alone, class B (CQ+) neurons respond to chloroquine alone, and class C (His+, CQ+) neurons respond to both histamine and chloroquine. The class A and class B cells are heterogeneous and can be divided based on the expression of TrpV1 and TrpA1, respectively, whereas class C cells are more homogeneous in terms of Trpv1 and bradykinin receptor expression. Using different ligands for voltage-gated sodium channels we have also identified expression of Nav1.7 and Nav1.8 in the different cell classes of DRG neurons that are sensitive to the pruritogens histamine and chloroquine.

Introduction

Each locus in the nervous system contains neurons with different set of properties (Franco and Müller 2013; Nelson et al. 2006; Sugino et al. 2006). Since a particular anatomical locus in the nervous system is involved in various physiological functions, it is expected that there exist a multitude of neuronal populations with varying patterns of ion channel and receptor expression in a given anatomical locus. The identification of these neuronal populations and the

corresponding constellation of ion channels and receptors expressed in these populations are important for the thorough understanding of their physiological function, and for monitoring changes in these populations as a function of ageing and the progression of pathological conditions.

The dorsal root ganglion (DRG) contains the cell bodies of neurons that send nerve projections into the periphery where they are activated by various chemical and mechanical stimuli. The activation of these nerves leads to different modes of somatosensation such as heat, cold, pain, and itch (Basbaum et al. 2009; Delmas et al. 2011). Since DRG neurons can detect a variety of somatosensory modalities, it follows that the cell types in a population of DRG neurons is extremely complex. It is estimated that there are >25 different cell types in DRG neurons (Teichert et al. 2012a).

One of the cell types of DRG neurons are the pruriceptors which detect itch and these cells are activated by pruritogens (itch-causing compounds) (LaMotte et al. 2013). Itch is defined as an unpleasant sensation that causes the reflex to scratch (Tominaga and Takamori 2013; Wilson and Bautista 2013; Yosipovitch et al. 2003). Itch can be acute, for example, an itch caused by an insect bite or chronic itch like in the case of people who suffer from atopic dermatitis (Ikoma et al. 2006; Paus et al. 2006). Severe cases of chronic itch greatly reduce the quality of life of people who suffer from the condition (Carr et al. 2013; Kini et al. 2011; Yosipovitch et al. 2003). Majority of itch conditions are associated with pathologies in the skin, however, itch can also be a symptom of organ pathologies such as some forms of liver disease or kidney failure (Belghiti

et al. 2013; Combs et al. 2015; Kremer et al. 2014; Mettang and Kremer 2015).

Itch is classified into two types: histamine-dependent itch and histamine-independent itch (Roberson et al. 2013; Akiyama et al. 2014). Histamine induces itch primarily through the activation of the H1R receptor (Shim and Oh 2008; Rossbach et al. 2011). Chloroquine an antimalaria drug, acting through the Mrgpra3 receptor induces histamine-independent itch (Liu et al. 2009; Wilson et al. 2011). There is limited information about mechanisms involved in the sensation of itch especially those mediated by the histamine-independent pathway (Jeffry et al. 2011). The identification and characterization of neuronal populations that respond to pruritogens are one of the important steps needed for a clearer understanding of the mechanisms that mediate itch.

Here we report the identification of three major subclasses of pruriceptors in the mouse DRG neurons. Class A responds to histamine (His+), class B responds to chloroquine (CQ+), and class C responds to both histamine and chloroquine (His+, CQ+). These pruritogen-sensitive cell classes are mostly small to medium diameter neurons and they make up a very small percentage of neurons in the DRG. Results from our experiments revealed the expression of receptors that are associated with nociception in the different subpopulation of pruritogens. We also report on the expression of Nav1.7 and Nav1.8 in these cell classes. Our research has identified cellular markers that can refine the definition of the pruriceptor class. These molecular markers serve an important role in the mechanistic understanding of itch. Moreover, the molecules identified in this research are potential therapeutic targets for the treatment of itch.

Materials and methods

Calcium imaging. The protocols for experiments using mice were approved by the Institutional Animal Care and Use Committee (IACUC) of the University of Utah. Methods for the culture of dorsal root ganglion (DRG) neurons have been described previously. Briefly, lumbar DRG's from adult CD1 mouse expressing green-fluorescent protein (GFP) conjugated to the calcitonin gene-related peptide (CGRP) were pooled and the cells dissociated and cultured overnight. FURA-2-AM dye was allowed to permeate the cells for 1 h. During the experiment the dye was excited alternately with 340- and 380-nm light and the emission from both excitations was monitored at 510 nm. The ratio of fluorescence intensity (340/380) is a measure of the cytosolic calcium. Results from these experiment is calcium imaging graph where the Y-axis represent the 340/380 ratio and the X-axis represent time in minutes. Specific times when a pharmacological agent is added are marked by arrows. Horizontal bars mark duration of the incubation of cells with the specified pharmacological agent.

Cellular profiling of histamine and chloroquine sensitive neurons. The cell culture was first depolarized by the addition of 30 mM KCl in 1x DRG observation solution (145 mM NaCl, 5 mM KCl, 2 mM $CaCl_2$, 1 mM $MgCl_2$, 1 mM sodium citrate, 10 mM glucose, 10 mM HEPES, and 1X penstrep) to identify neurons. After depolarization, the cells were challenged by the sequential application of different pharmacological agents every 5 min. The compounds were added in the following sequence: histamine (100 mM), chloroquine (1 mM), 4 ºC bath, bradykinin (10 mM), menthol (400 mM), AITC (100 mM), and capsaicin

(300 nM). Histamine, chloroquine, 4 ºC bath and bradykinin were incubated with the cells for 30 s while the other reagents were incubated with the cells for 10 s. All reagents were purchased from Sigma (St. Louis, MO, USA). A summary of the reagents used in these experiments are shown in Table 4.1.

Voltage-gated sodium channels in His+, Caps+ and CQ+, AITC+ neurons. The experiment was started by the addition of 100 μM histamine. The cells were then washed and after 5 min, 1 mM chloroquine was added to the cells. After the chloroquine addition, the cells were depolarized three times with 20 mM KCl at 5-min-intervals. After the third KCl pulse, 1 μM tetrodotoxin (TTX) in 1X DRG observation solution was added to the cells. After 4 min this solution was replaced with another solution containing 20 μM veratridine and 1 μM TTX. After 1 min the cells were depolarized with a solution containing 20 mM KCl, 20 μM veratridine, and 1 μM TTX. The cells were then washed and depolarized twice with 20 mM KCl every 5 min. Throughout this phase of the experiment, the cells were incubated with 1 μM TTX. After these depolarizations, the 1 μM TTX solution was replaced 10 μM μ-PIIIA. After 4 min, the μ-PIIIA solution was replaced and the cells incubated for 1 minute with a solution containing 20 μM veratridine, and 10 μM μ-PIIIA. After 1 min, the cells were depolarized by a solution containing 20 mM KCl, 20 μM veratridine, and 10 μM μ-PIIIA. The cells were finally depolarized twice every 5 min while maintaining the μ-PIIIA concentration. After the final depolarization, menthol, AITC, and capsaicin were sequentially added to the cells every 5 min. Relevant information about the reagents used in these experiments are shown in Table 4.1.

Results

Dorsal root ganglion (DRG) neurons from CD1 mouse heterologously expressing green fluorescent protein (GFP) marker conjugated to the calcitonin gene related peptide (CGRP) were dissociated and cultured overnight. CGRP is a marker for peptidergic nociceptors (McCoy et al. 2013), hence, neurons displaying the green fluorescence of GFP belong to the peptidergic nociceptor class. The cells were also stained with antibodies against isolectin B4 (IB4) to identify neurons that belong to the nonpeptidergic nociceptor class (Franck et al. 2011). A total of 5099 neurons were examined based on their responses to various challenges in the calcium imaging experiments. Histamine and chloroquine were used to identify the putative pruriceptors. The cells were also challenged with 4 ºC bath as well as bradykinin, menthol, AITC, and capsaicin to determine whether the pruriceptor class also coexpresses the receptors of these challenge compounds. Another experiment determined the expression of voltage-gated sodium channel using veratridine, tetrodotoxins (TTX) and the conotoxin μ-PIIIA. The compounds used in these experiments and their corresponding molecular targets are listed in Table 4.1.

The pruriceptors comprise a very small percentage of neurons in the DRG. Histamine and chloroquine were used to identify the cells expressing the histamine and chloroquine receptor. Activation of the H1R receptor by histamine and the MrgprA3 receptor by chloroquine was shown to induce symptoms associated with itch (Shim and Oh 2008; Rossbach et al. 2011; Liu et al. 2009; Wilson et al. 2011). Application of 100 μM histamine and 1 mM chloroquine in the

same experiment elicited a robust increase in cytosolic calcium in a small number of neurons in the experiment. Our experiments showed predominantly divergent expression of the histamine and chloroquine receptors. Cells that respond to histamine alone belong to class A (His+ cells) whereas cells that respond to chloroquine are class B cells (CQ+ cells). There is, however, a very small number of neurons belonging to class C (His+, CQ+) cells that express the receptors for both histamine and chloroquine. Experiments conducted on 5099 neurons prepared from three adult mice showed that 3% of neurons belong to class A (His+), 9% of neurons are in class B (CQ+), and 1% of neurons are class C (His+, CQ+ cells) (Figure 4.1B). Interestingly, these cell classes responding to pruriceptors contain both peptidergic and nonpeptidergic nociceptors. The class A (His+), class B (CQ+), and class C (His+, CQ+) classes contains 30%, 39%, and 32% peptidergic nociceptors, respectively. The nonpeptidergic neurons comprise 53% of the class A (His+) cells, 61% of the class B (CQ+) cells, and 43% of the class C (His+, CQ+) cells. Representative calcium imaging traces of cells in these pruriceptor classes are shown in Figure 4.1A.

The pruriceptors also express markers for nociceptive neurons. Bradykinin (bradykinin receptor agonist), allyl isothiocyanate (AITC) (TrpA1 agonist), and capsaicin (TrpV1 agonist) are markers for nociceptive neurons (Cayla et al. 2012; Rashid et al. 2004; Miyamoto et al. 2009; Viana 2016; Julius 2013). Further, it was shown that TrpV1 is required for histamine-dependent (Shim et al. 2007) itch while TrpA1 is required for histamine-independent itch

(Wilson et al. 2011). Individual applications of bradykinin, AITC, and capsaicin elicited a response in a subset of cell populations that are sensitive to histamine and chloroquine. 51.0 ± 4.2% of cells in class A respond to capsaicin while the remainder of the cells are insensitive to capsaicin. In class B cells (CQ+), 50.0 ± 2.4% respond to AITC while the rest of the cells in class B did not respond to AITC. Given these results, the class A cells (His+) could be further subdivided into the His+, Caps+ subclass, and the His+, Caps- subclass while the class B cells (CQ+) could be further subdivided into the CQ+, AITC+ subclass, and CQ+, AITC- subclass. Since TrpV1 the capsaicin target is required for histamine-dependent itch while the AITC target TrpA1 is required for histamine-independent itch, it is interesting that not all the cells in class A (His+) respond to capsaicin and not all cells in class B (CQ+) respond to AITC. Thus, the His+, Caps+ cells in class A and the CQ+, AITC+ cells in class B mediates itch through the previously identified TrpV1-dependent (histamine-dependent) and TrpA1-dependent (histamine-independent) mechanisms, respectively. Surprisingly the class C cells (His+, CQ+) cells are more homogeneous than either of the cells in class A or class B. In class C cells (His+, CQ+), 73.0 ± 7.4% respond to bradykinin and 92 ± 4.5% of these cells also respond to capsaicin. These data suggest that class C cells mediate itch through the histamine-dependent mechanism. Although the possibility that class C cells mediate itch through the histamine-indpendent mechanism cannot be ignored at this point.

Voltage-gated sodium channels in His+, Caps+ cells, and CQ+, AITC+ cells. Combinations of pharmacological agents were used to specifically

activate voltage-gate sodium channel (VGSC) isoforms in the different classes of pruriceptors. These experiments were performed by the sequential application into the DRG neurons of veratridine and tetrodotoxin (TTX) and veratridine and the conotoxin μ-PIIIA. Veratridine is a compound that activates voltage-gated sodium channel while TTX and μ-PIIIA selectively inhibit specific VGSC isoforms. The combination of TTX and veratridine inhibits TTX-sensitive VGSC and activate TTX-resistant VGSC while the combination of veratridine and μ-PIIIA will only activate Nav1.7 and TTX-resistant VGSC and inhibit the rest of the neuronal TTX-sensitive VGSC. Previously, Teichert et al. (2012b) showed that the combination of TTX and veratridine activates Nav1.8. Thus, the application veratridine and TTX will identify Nav1.8 while the application of veratridine and μ-PIIIA will identify Nav1.8 and Nav1.7. Sample calcium imaging traces for these experiments are shown in Figure 4.2A.

Analysis of the experiments showed that a percentage of the cells in class A, class B, and class C showed amplification of the cytosolic calcium concentration when depolarized by KCl in the presence veratridine and TTX suggesting the expression of Nav1.8. Depolarizing the cells in the presence of veratridine and μ-PIIIA elicited a higher increase in cytosolic calcium in a percent of cells in each class when compared to the previous depolarization in the presence of veratridine and TTX suggesting the expression of Nav1.7. Quantifying the results from these experiments showed that 45.7 ± 5.8% and 72.3 ± 2.3% of cells in class A express Nav1.8 and Nav1.7, respectively. In class B cells, 52.0 ± 2.9% express Nav1.8 and 64.0 ± 7.2% express Nav1.7. In class C

cells, 36.7 ± 5.9% express Nav1.8 and 85.0 ± 4.5% express Nav1.7. These results are shown in Figure 4.2B.

Discussion

Constellation pharmacology is an experimental paradigm that uses calcium imaging to determine the expression of ion channels and receptors in a particular cell class. The identification of ion channel and receptor expression is achieved by the sequential application of pharmacological agents called challenge compounds to a culture of cells. The receptor agonist challenge uses specific receptor agonists to elicit a response from the cells while the membrane potential challenge uses ligands of voltage-gated ion channels which could either activate or inhibit the channels when the membrane is depolarized. The application of different challenge compounds into a culture of dorsal root ganglion (DRG) neurons elicits a wide array of responses. Cells that have the same response profile are classified into specific cell classes/types. Using the constellation pharmacology paradigm, Teichert et al. (2012b) has successfully identified subclasses of neurons in the mouse DRG.

Here we used constellation pharmacology to identify cellular subclasses that are responsive to the pruritogens histamine and chloroquine. Histamine defines histamine-dependent itch whereas chloroquine defines histamine-independent itch. Considering that there are two general classifications of itch we designed experiments to test whether different cell populations are sensitive to histamine and chloroquine. Our experiments revealed three cell classes that

respond to the pruritogens. One class we call class A respond to histamine alone, the class B cells respond to chloroquine alone, and the class C respond to both histamine and chloroquine. Interestingly, the pruritogen responsive population contains cells that are either positive for CGRP and/or IB4, suggesting that these populations contain cells belonging to the peptidergic nociceptor and nonpeptidergic nociceptor classes. These results indicate the heterogeneity of the cellular classes in the DRG that are sensitive to the pruritogens.

Cell classes A and B have an added level of heterogeneity in terms of the expression of Trp channels previously shown to be important for histamine-dependent and histamine-independent itch. Class A cells can be further subdivided into the capsaicin sensitive (His+, Caps+) and capsaicin insensitive (His+, Caps-), whereas the class B cells can be further divided into the AITC sensitive (CQ+, AITC+) and AITC insensitive (CQ+, AITC-) subclasses. Research has previously shown that TrpV1 the capsaicin receptor is required for histamine-dependent itch while the AITC receptor TrpA1 is required for histamine-independent itch (Shim et al. 2007; Wilson et al. 2011). These results indicate two possibilities in terms of the cell classes that detect itch. One possibility is that only the His+, Caps+ and CQ+, AITC+ subclasses are the pruriceptors while the other subclasses His+, Caps- and CQ+, AITC- are possibly involved in other modes of somatosensation. Another possibility is that all the His+ and CQ+ cells are pruriceptors, however, the His+, Caps- class and the CQ+, AITC- cells mediate itch in a mechanism that does not require TrpV1 and TrpA1, respectively.

Interestingly, the class C cells which comprise the smallest population of pruritogen-sensitive neurons is generally homogeneous. The majority of the cells in this class express the bradykinin receptor (BkR) and TrpV1. Thus, class C cells can mediate itch through the histamine-dependent mechanism that requires TrpV1. The expression of the BkR in this class is unexpected considering that bradykinin receptor is associated with nociceptors. However, reports showed that bradykinin the ligand for BkR is a pruritogen when applied to skin lesions in atopic dermatitis (AD) (Hosogi et al. 2006), thus, in atopic dermatitis, BkR mediates itch. The data presented by Hosogi et al. (2006) together with our experimental results suggest that class C cells is the potential pruriceptor that is involved in the itching caused by bradykinin in AD. Moreover, these data suggest that inhibitors of BkR can potentially be explored for the treatment of itch in atopic dermatitis.

Membrane potential challenge was used to identify the expression of voltage-gated sodium channels (VGSC) in the cell classes identified in this research. A combination of VGSC agonist and antagonist elicited responses indicative of the expression Nav1.8 and Nav1.7. The Nav1.8 expression was determined from the response of the cells upon depolarization by KCl in the presence of veratridine and tetrodotoxin (TTX). In the same experiment, TTX and the conotoxin μ-PIIIA (10 μM) were applied after washing veratridine. The concentration of μ-PIIIA used in these experiments would inhibit neuronal VGSC's except Nav1.7, therefore, the increase in cytosolic calcium concentration is a result of the activation of both Nav1.8 and Nav1.7. Thus, the higher increase

in cytosolic calcium concentration in response to the application of μ-PIIIA and TTX when compared to the application of veratridine and TTX suggest the expression of Nav1.7.

Results from the experiment showed that all the cell classes predominantly express Nav1.7. Class C cells (His+, CQ+) has the largest percentage of cells expressing Nav1.7 class B cells has lowest Nav1.7 expression. Nav1.8 is not expressed to the same extent as Nav1.7. The highest Nav1.8 expression is found in class B cells while class C cells have the least Nav1.8 expression. The broad expression of Nav1.7 across all cell classes we have identified in this research suggests the involvement of Nav1.7 in both the histamine-dependent and histamine-independent itch. Our conclusion regarding the involvement of Nav1.7 in itch is in agreement with the experimental results by Devigili et al. (2014) which showed that a gain of function mutation in Nav1.7 causes paroxysmal itch. Our data further suggest that specific inhibitors of Nav1.7 are potential drugs for the treatment of both histamine-dependent and histamine-independent itch. Lee et al. (2014) has shown that the inhibition of Nav1.7 by a monoclonal antibody specific to Nav1.7 attenuates both histamine-dependent and histamine-independent itch. Presumably the monoclonal antibody targets Nav1.7 which is predominantly expressed in the cell classes we have identified here.

In this research we have identified classes of DRG neurons that are responsive to the pruritogens histamine and chloroquine. The three classes of cells we have identified in this research mirror the complexity of pruriception in

which different mechanisms were shown to mediate itch. The class A and class C cells which are histamine sensitive presumably mediates itch through the histamine dependent mechanism, whereas class B and class C cells mediate itch through the histamine-independent mechanism.

Our data point to an underlying complexity in an already complex mode of somatosensation which is itch. Approximately 50% of the cells in classes A and B express the receptors shown to be required for itch. Thus, only half of cells in these cell classes mediate itch under the canonical TrpV1- and TrpA1-mediated mechanism. However, Han et al. (2013) showed that MrgprA3-expressing neurons are a labelled line specific for itch. Moreover TrpV1 and TrpA1 knock-out did not completely abolish both histamine-dependent and histamine-independent itch, respectively (Shim et al. 2007; Wilson et al. 2011). These data suggest that there is an unknown mechanism of sensing itch that is independent of TrpV1 and TrpA1. Our research has identified the possible cell classes that mediate itch in a mechanism that neither requires TrpV1 in histamine-dependent itch nor TrpA1 in histamine-independent itch.

Class C cells express both the histamine receptor and MrgprA3. This cell class predominantly expresses Trpv1, thus, cells in this class mediate itch in a histamine-dependent mechanism that requires TrpV1. Interestingly, a small percent of cells in this class expresses TrpA1, thus, only these cells mediate histamine-independent itch that requires TrpA1. However, chloroquine was shown to sensitize TrpV1 (Than et al. 2013) suggesting that itch could also be mediated by the coupling of MrgprA3 and TrpV1 in cells that coexpress MrgprA3

and TrpV1.

The tailored therapeutic strategy for targeting specific neuronal subtypes involved in pathologies is one of the immediate applications of constellation pharmacology. This is illustrated by the potential use of bradykinin receptor antagonist for the treatment of itch in atopic dermatitis. Another application of classifying cell classes and cataloging ion channel and receptor expression is the ability to monitor changes in these cell classes as a function of disease or ageing. Our results for the different pruriceptor class serve as a baseline for comparison of the changes in these cell classes. Importantly, we have identified cell classes such as the capsaicin negative cells in class A and AITC negative cells in class B that potentially mediate itch in a mechanism that does not require TrpV1 and TrpA1. Future research should focus on these cell classes for a more comprehensive understanding of why we itch and what we can do to treat itch.

Figure 4.1. **Responses of DRG neurons to the application of histamine and chloroquine and other challenge compounds**. A) Sample calcium imaging traces showing the response profile of the three major classes of neurons responding to the pruritogens histamine and chloroquine. Each trace represents a single cell in the experiment. The Y-axis represents the ratio of the emission at 340 nm and 380 nm (340/380) while the X-axis represents time and the specific time point where a challenge compound is added is marked by an arrow. Each upward deflection in the graph represents a response to a specific challenge compound. The top 3 panels represents the class A (His+) cells, the middle three panels represent the class B (CQ+) cells, and the bottom 3 panels represent the class C (His+, CQ+) cells. These traces also shown the response of the cells to capsaicin, AITC and bradykinin **B)** Quantification of the percentage of cells in each major pruritogen-sensitive population responding to a specific challenge compound. The experiments showed that class A (His+), class B (CQ+), and class C (His+,CQ+) cells comprise 3%, 9% and 1% respectively of the total DRG neuron population. The percentage cells that do not respond to histamine and chloroquine (class D) are also shown.

A

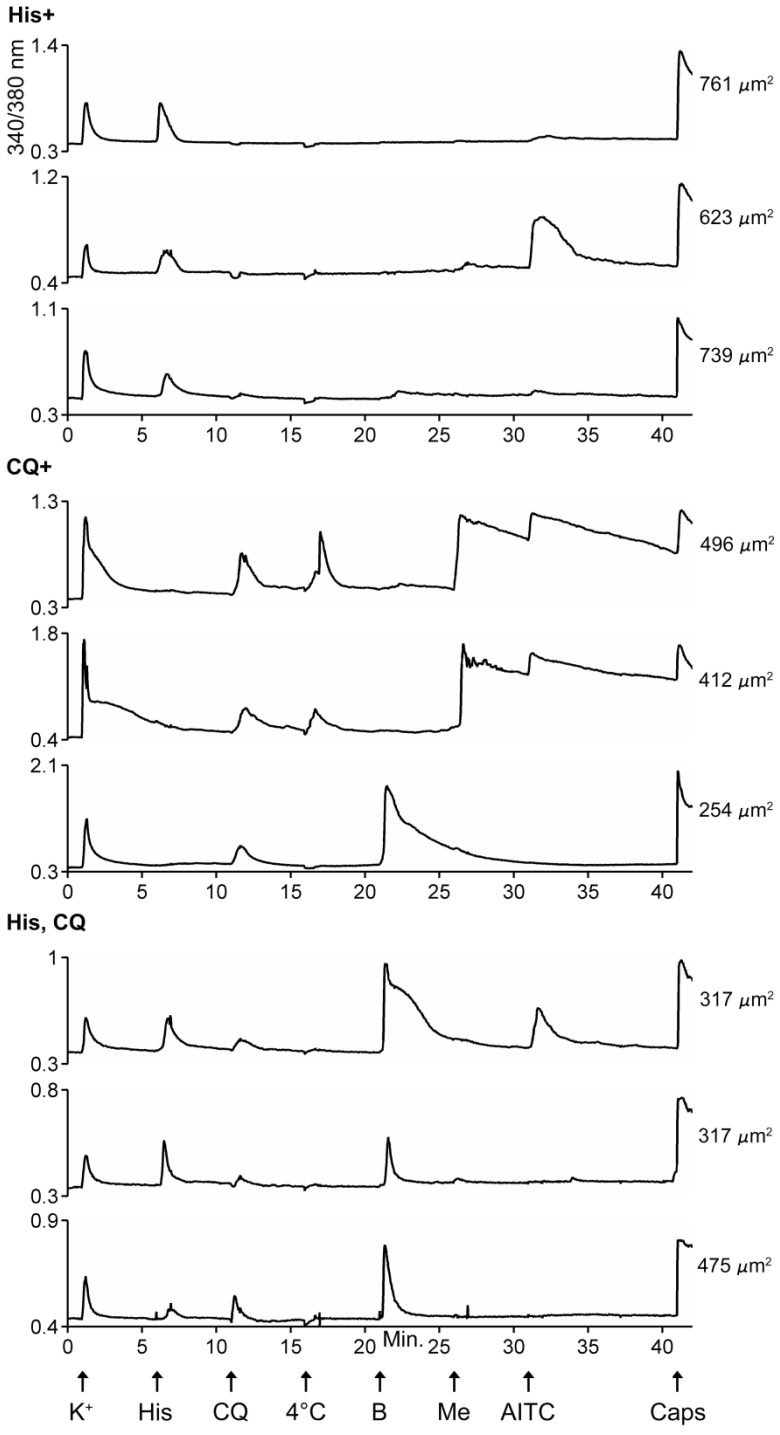
His+
340/380 nm
761 μm²
623 μm²
739 μm²
CQ+
496 μm²
412 μm²
254 μm²
His, CQ
317 μm²
317 μm²
475 μm²
Min.
K⁺
His
CQ
4°C
B
Me
AITC
Caps

B

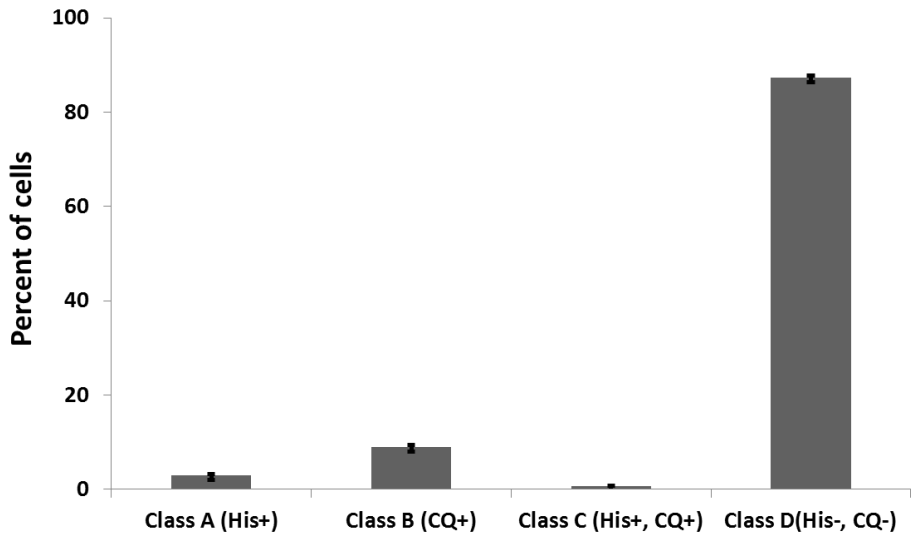

Figure 4.1. Continued

Figure 4.2. Voltage-gated sodium channel (VGSC) expression in the class A (His+) cells, class B (Caps+) cells and in class C (CQ+, AITC+) cells. A) Sample calcium imaging trace for the experiment to identify expression of Nav1.7 and Nav1.8 in the different classes of prurifeptors. The top panel show representative trace of the class A (His+) cells, the middle panel shows a representative trace of the class B (CQ+) cells and the bottom panel shows a representative trace of the class C (His+, CQ+) cells. The cells were depolarized by the application of 20 mM KCl. The application of TTX and veratridine amplifies the response from TTX-resistant Nav1.8 VGSC while the application of TTX and μ-PIIIA amplifies the response from Nav1.8 and Nav1.7. The time intervals when TTX and μ-PIIIA is incubated with the cells is marked by the solid black line while the time interval of veratridine incubation is marked by the solid gray line. The results of the experiments are quantified in B. 72.3 ± 2.3% of cells in class A express Nav1.7 while 45.7 ± 5.8% express Nav1.8. In class B cells, 64.0 ± 7.2% express Nav1.7 and 52.0 ± 2.9% express Nav1.8. In class C cells, 85.0 ± 4.5% of cells express Nav1.7 and 36.7 ± 5.9% express Nav1.8

A

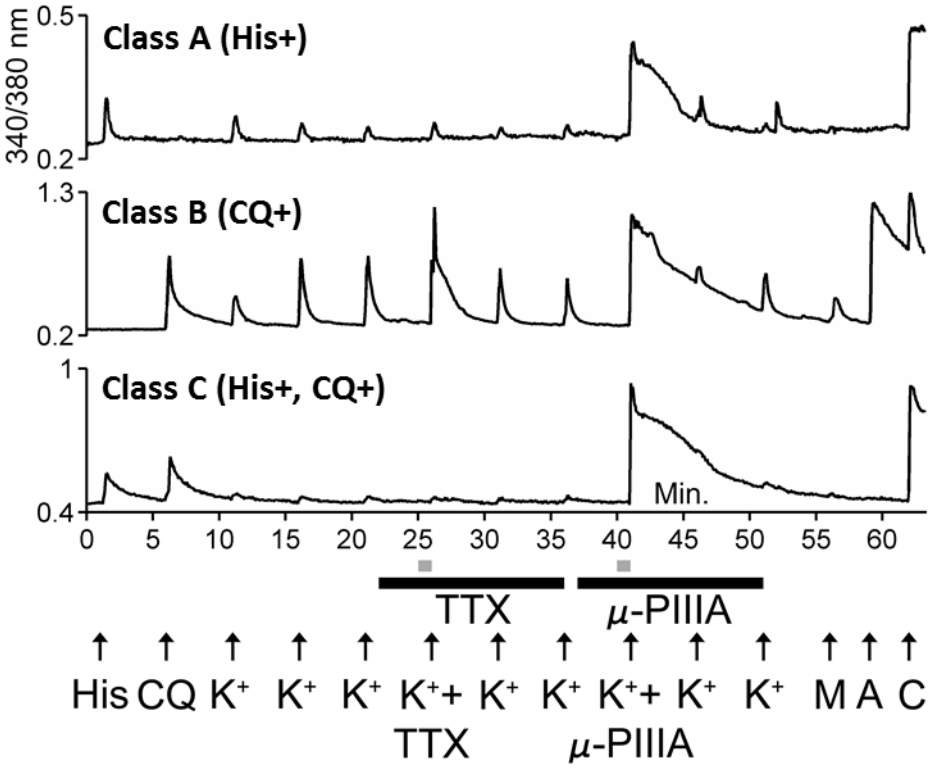
340/380 nm
0.5
0.2
Class A (His+)
1.3
0.2
Class B (CQ+)
1
0.4
Class C (His+, CQ+)
Min.
0 5 10 15 20 25 30 35 40 45 50 55 60
TTX
μ-PIIIA
His CQ K+ K+ K+ K++ K+ K+ K++ K+ K+ M A C
TTX
μ-PIIIA

B

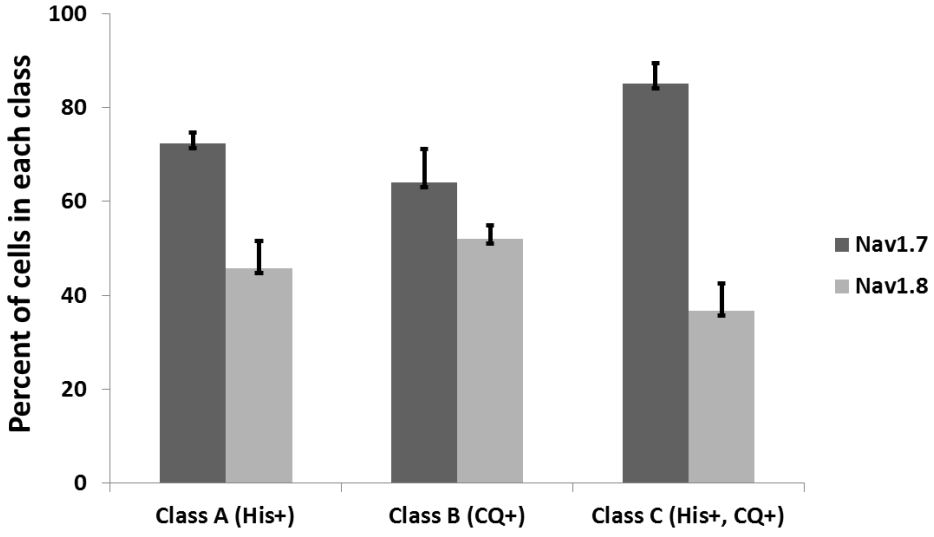
Percent of cells in each class
100
80
60
40
20
0
Class A (His+)
Class B (CQ+)
Class C (His+, CQ+)
Nav1.7
Nav1.8

Table 4.1. Challenge compounds used in experiments conducted in this research.

Compound	Abbreviation	Target	Concentration
Histamine	**His**	**Histamine receptor**	**100 μM**
Chloroquine	**CQ**	**MrgprA3**	**1 mM**
Bradykinin	**B**	**Bradykinin receptor**	**10 μM**
Menthol	**Me/M**	**TrpM8**	**400 μM**
Allyl isothiocyanate	**AITC/A**	**TrpA1**	**100 μM**
Capsaicin	**Caps/C**	**TrpV1**	**300 nM**
Tetrodotoxin	**TTX**	**VGSC**	**1 μM**
Veratridine	**Ver**	**VGSC**	**20 μM**
μ-PIIIA	**μ-PIIIA**	**VGSC**	**10 μM**

References

Akiyama T, Tominaga M, Takamori K, Carstens MI, Carstens E. 2014. Roles of glutamate, substance-P and gastrin releasing-peptide as spinal neurotransmitters of histaminergic and nonhistaminergic itch. Pain 155(1): 80-92.

Basbaum AI, Bautista DM, Scherrer, Julius D. 2009. Cellular and molecular mechanisms of pain. Cell 139(2): 267-284.

Bautista DM, Siemens J, Glazer JM, Tsuruda PR, Basbaum AI, Stucky CL, Jordt SE. Julius D. 2007. The menthol receptor TrpM8 is the principal detector of environmental cold. Nature 448(7150): 204-208.

Belghiti M, Estevez-Herrera J, Gimenez-Garzo C, Gonzalez-Usano A, Montoliu C, Ferrer-Montiel A, Felipo V, Planells-Cases R. 2013. Potentiation of the transient receptor potential vanilloid 1 channel contributes to pruritogenesis in a rat model of liver disease. J Biol Chem. 288(14): 9675-9685.

Carr CW, Valedar E, Chen SC. 2014. Factors mediating the impact of chronic pruritus on quality of life. JAMA Dermatol. 150(6): 613-620.

Cayla C, Labuz D, Malcheska H, Bader M, Schäfer M, Stein C. 2012. Impaired nociception and peripheral opioid antinociception in mice lacking both kinin B1 and B2 receptors. Anesthesiology 116(2): 448-457.

Combs SA, Teixeira JP, Germain MG. 2015. Pruritus in kidney disease. Semin Nephrol. 35(4): 383-391.

Delmas P, Hao J, Rodat-Despoix L. 2011. Molecular mechanisms of mechanotransduction in mammalian sensory neurons. Nat Rev Neurosci. 12(3): 139-153.

Devigili G, Eleopra R, Pierro T, Lombardi R, Rinaldo S, Lettieri C, Faber CG, Merkies IS, Waxman SG, Lauria G. 2014. Paroxysmal itch caused by a gain-of-function Nav1.7 mutation. Pain 155(9): 1702-1707.

Franck MC, Stenqvist A, Li L, Hao J, Usoskin D, Xu X, Wiesenfel-Hallin Z, Ernfors P. 2011. Essential role of Ret for defining non-peptidergic nociceptor phenotypes and functions in adult mouse. Eur J Neurosci. 33(8): 1385-1400.

Franco SJ, Müller U. 2013. Shaping our minds: Stem and progenitor cell diversity in the mammalian neocortex. Neuron 77(1): 19-34.

Hosogi M, Schmelz M, Miyachi Y, Ikoma A. 2006. Bradykinin is a potent pruritogen in atopic dermatitis: a switch from pain to itch. Pain 126(1-3): 16-23.

Ikoma A, Steinhoff M, Stander S, Yosipovitch G, Schmelz M. 2006. The neurobiology of itch. Nat Rev Neurosci. 7(7): 535-547.

Jeffry J, Kim S, Chen ZF. 2011. Itch signaling in the nervous system. Physiology 26(4): 286-292.

Julius D. 2013. Trp channels and pain. Annu Rev Cell Dev Biol. 29: 355-384.

Kini SP, DeLong LK, Valedar E, McKenzie-Brown AM, Schaufele M, Chen SC. 2011. The impact of pruritus on the quality of life: the skin equivalent of pain. Arch Dermatol. 147(10): 1153-1156.

Knowlton WM, Palkar R, Lippoldt EK, McCoy DD, Baluch F, Chen J, McKemmy DD. 2013. A sensory-labelled line for cold: TRPM8-expressing sensory neurons define the cellular basis for cold, cold pain and cooling-mediated analgesia. J Neurosci. 33(7): 2837-2848.

Kremer AE, Feramisco J, Reeh PW, Beuers U, Oude Elfirink RP. 2015. Receptors, cells and circuits involved in pruritus of systemic disorders. Biochim Biophys Acta 1842(7): 869-892.

LaMotte RH, Dong X, Ringkamp M. 2013. Sensory neurons and circuits mediating itch. Nat Rev Neurosci. 15(1): 19-31.

Lee JH, Park CK, Chen G, Han Q, Xie RG, Liu T, Ji RR, Lee SY. 2014. A monoclonal antibody that targets a Nav1.7 voltage sensor for pain and itch relief. Cell 157(6): 1393-1404.

Liu Q, Tang Z, Surdenikova L, Kim S, Patel KN, Kim A, Ru F, Guan Y, Weng HJ, Geng Y, Undem BJ, Kollarik M, Chen ZF, Anderson DJ, Dong X. 2009. Sensory neuron-specific GPCR Mrgprs are itch receptor mediating chloroquine-induced pruritus. Cell 139(7): 1353-1365.

McCoy ES, Taylor-Blake B, Street SE, Pribisko AL, Zheng J, Zylka MJ. 2013. Peptidergic CGRPα primary sensory neurons encode heat and itch and tonically suppress sensitivity to cold. Neuron 78(1): 138-151.

Mettang T, Kremer AE. 2015. Uremic pruritus. Kidney Int. 87(4): 685-691.

Miyamoto T, Dubin AE, Petrus MJ, Patapoutian A. 2009. TrpV1 and TrpA1 mediate peripheral nitric oxide-induced nociception in mice. PlosOne 4(10): e7596.

Nelson SB, Sugino K, Hempel CM. 2006. The problem of neuronal cell types: A physiological genomics approach. Trends Neurosci. 29(6): 339-345.

Paus R, Schmelz M, Biro T, Steinhoff M. 2006. Frontiers in pruritus research: scratching the brain for more effective itch therapy. J Clin Invest. 116(5): 1174-1186.

Rashid MH, Inoue M, Matsumoto M, Ueda H. 2004. Switching of bradykinin-mediated nociception following partial sciatic nerve injury in mice. J Pharmacol Exp Ther. 308(3): 1158-1164.

Roberson DP, Gudes S, Sprague JM, Patoski HA, Robson VK, Blasl F, Duan B, Oh SB, Bean BP, Ma Q, Binshtok AM, Woolf CJ. 2013. Activity-dependent silencing reveals functionally distinct itch-generating sensory neurons. Nat Neurosci. 16(7): 910-919.

Rossbach K, Nassenstein C, Gschwandtner M, Schnell D, Sander K, Seifert R, Stark H, Kietzmann M, Bäumer W. 2011. Histamine H1, H3 and H4 receptors are involved in pruritus. Neuroscience 190: 80-102.

Shim WS, Oh U. 2008. Histamine-induced itch and its relationship with pain. Mol Pain 4:29.

Shim WS, Tak MH, Lee MH, Kim M, Kim M, Koo JY, Lee CH, Kim M, Oh U. 2007. TrpV1 mediates histamine-induced itching via the activation of phospholipase A2 and 12-lipoxygenase. J Neurosci. 27(9): 2331-2337.

Sugino K, Hempel CM, Miller MN, Hattox AM, Shapiro P, Wu C, Huang CJ, Nelson SB. 2006. Molecular taxonomy of major neuronal classes in the adult mouse forebrain. Nat Neurosci. 9(1): 99-107.

Tamura S, Morikawa Y, Senba E. 2005. TrpV2 a capsaicin receptor homologue, is expressed predominantly in the neurotrophin-3-dependent subpopulation of primary sensory neurons. Neuroscience 130(1): 223-228.

[a]Teichert RW, Smith NJ, Raghuraman S, Yoshikami D, Light AR, Olivera BM. 2012. Functional profiling of neurons through cellular neuropharmacology. Proc Natl Acad Sci. 109(5): 1388-1395.

[b]Teichert RW, Raghuraman S, Memon T, Cox JL, Foulkes T, Rivier JE, Olivera BM. 2012. Characterization of two neuronal subclasses through constellation pharmacology. Proc Natl Acad Sci. 109(31): 12758-12763.

Than JY, Li , Hasan R, Zhang X. 2013. Excitation and modulation of TrpA1, trpV1 and TrpM8 channel-expressing sensory neurons by the pruritogen chloroquine. J Biol Chem. 288(18): 12818-12827.

Tominaga M, Takamori K. 2013. An update on peripheral mechanisms and treatment of itch. Biol Pharm Bull. 36(8): 1241-1247.

Viana F. 2016. TrpA1 channels: molecular sentinels of cellular stress and tissue damage. J Physiol. 594(15): 4151-4169.

Wilson SR, Bautista D. 2013. Itching for relief. Nat Neurosci. 16(7): 775-777.

Wilson SR, Gerhold KA, Bifolck-Fisher A, Liu Q, Patel KN, Dong X, Bautista DM. 2011. TRPA1 is required for histamine-independent, Mas-related G protein-coupled receptor-mediated itch. Nat Neurosci. 14(5): 595-602.

Yosipovitch G, Greaves MW, Schmelz M. 2003. Itch. Lancet 361(9358): 690-694.

CHAPTER 5

SUMMARY

In this research, novel vertebrate-active conotoxins were identified from cone snail clades with very limited toxinological information. These conotoxins were discovered using the norepinephrine transporter (NET) uptake assay and calcium imaging. These assays were never before used for conotoxin discovery. Chapter 2 describes conotoxins purified from the venom of cone snails from different mollusk-hunting clades using the NET uptake assay. Chapter 3 describes conotoxins purified using calcium imaging and identified from a clade of worm-hunting cone snails. The major driving force for the efforts to discover novel conotoxins is the research and therapeutic applications of these compounds. Chapter 4 described a research project where a conotoxin was one of the pharmacological compound used to identify ion channels and receptors expressed by a small population of dorsal root ganglion (DRG) neurons that are sensitive to pruritogens (itch-causing compounds).

Pharmacologically distinct peptides in the T-superfamily

The conotoxins described in Chapter 2 were all purified from mollusk-hunting cone snails and belong to the T-superfamily. These conotoxins share the same pattern of disulfide bonds, however, the biological activities of these conotoxins in mice indicate they belong to different pharmacological families. Two of these conotoxins χ-AoIC and χ-AuID inhibit the norepinephrine transporter (NET) and belong to the χ-conotoxin family. The conotoxin fv1a does not inhibit NET, however, this peptide is active in our assays. fv1a partially inhibits the cytosolic flux of calcium in a population of dorsal root ganglion (DRG)

neurons upon depolarization by KCl and elicits *in vivo* a hyperactive phenotype upon intracranial (IC) injection in mice.

The activity of χ-AoIC and χ-AuID against NET has medical significance since NET has been implicated in various neurological disorders (Bönisch and Brüsss 2006; Zhou 2004). It is important to note at this point that the first χ-conotoxin discovered χ-MrIA from *Conus marmoreus*, has gone through phase II clinical trial for the treatment of pain (Brust et al. 2009; Green et al. 2014), thus, the χ-conotoxins reported in this dissertation can also be explored for their application in the treatment of pain. The analgesic effect of NET inhibitors is shown to involve the activation of α2-adrenergic receptors in the descending pain pathway (Hajhashemi et al. 2014; Hall et al. 2011).

The conotoxin fv1a from *Conus furvus* (Calibanus clade) (Puillandre et al. 2014) is homologous to the the χ-conotoxins, however, this conotoxin does not inhibit NET. fv1a is biologically active *in vivo* in mice upon intracranial (IC) injection and displays partial inhibition of the cytosolic calcium increase in DRG neurons upon depolarization by KCl in calcium imaging experiments. Experiments conducted in this research indicate that fv1a is pharmacologically distinct from the χ-conotoxins, hence, fv1a belongs to a different conotoxin family.

The conotoxins χ-AoIC, χ-AuID and fv1a reported here and together with the previously characterized χ-MrIa allowed for the identification of amino acids important for the inhibitory activity of the χ-conotoxins against NET. Analysis of the sequence revealed that the amino acids flanked by the second and third

cysteines are conserved among the χ-conotoxins and highly divergent in fv1a (Figure 5.1). Thus, the amino acids -GYKL- are important for NET inhibition. Conservative substitution in these amino acids does not appear to be crucial for activity against NET. For example, the substitution of leucine with a methionine in χ-AoIC did not affect the activity of χ-AoIC to inhibit NET.

The discovery of related conotoxins with varying degrees of potency toward NET is important since these conotoxins can be used to identify the mechanism of NET inhibition. Knowing how these conotoxins inhibit NET can lead to the design of ligands that 1) would target NET with very high specificity and potency, and 2) have fewer side effects in cases they are used as drugs. For example, sequence comparison among the χ-conotoxins indicates that the leucine to methionine substitution in χ-AoIC appears to increase the potency of χ-AoIC to inhibit NET. Thus, it appears that a bigger more hydrophobic amino acid in this position would result to a more potent ligand that inhibits NET.

Glycine-rich conotoxins in the O1-superfamily

The O1-superfamily currently contains the most medically important conotoxin, ω-MVIIA. ω-MVIIA is a drug sold under the name Ziconotide (Prialt) for the treatment of pain. The inhibitory activity of this conotoxin against the voltage-gated calcium channel isoform Cav2.2 is the mechanism for its analgesic activity (Miljanich 2004). The O1-superfamily also contains conotoxins that target voltage-gated potassium channels (κ-conotoxins) (Shon et al. 1998) and voltage-gated sodium channels (δ- and μO-conotoxins) (Bulaj et al. 2000; McIntosh et al.

1995). Examples of these conotoxin families are given in Table 5.1. It is to be noted that most of these conotoxins were identified from the venom of fish-hunting cone snails. However this table does not imply that only fish-hunting cone snails are sources of vertebrate-active conotoxins belonging to the O1-superfamily. The worm-hunting cone snails comprise the largest group in Conus thus, worm hunters potentially hold a tremendous wealth of vertebrate-active conotoxins in the O1-superfamily.

The conotoxins described in Chapter 3 all belong to the O1-superfamily, and they were all identified from the Virgiconus clade of worm-hunting cone snails. The first conotoxin identified from this clade is vi6a from *Conus virgo*. vi6a causes a partial inhibition of the increase in cytosolic calcium in response to depolarization of DRG neurons by KCl in calcium imaging experiments. Intracranial (IC) and intraperitoneal (IP) injection of vi6a into young mice (17 – 21 days old) elicit hyperactivity.

A striking feature of vi6a is the unusual abundance of glycine residues. vi6a has 26 noncysteine residues and 11 of these 26 amino acids are glycines. A screen of the mRNA transcripts isolated from the venom ducts of *Conus virgo*, *Conus terebra,* and *Conus kintoki* which are also members of the Virgiconus clade revealed homologous conotoxins that are equally glycine-rich. Surprisingly, two glycine-rich conotoxins were further identified from *Conus virgo.* In total, 3 glycine-rich conotoxins were identified from *C. virgo*, two from *C. terebra,* and one from *C. kintoki*. *C. virgo* and *C. terebra* are shallow water species whereas *C. kintoki* is a deep water species, thus, it appears that the glycine-rich

conotoxins are expressed by members of the Virgiconus clade across a wide range of marine habitats.

The novel conotoxins described in this research appear to be distinct from previously described conotoxins in the O1-superfamily. A very obvious difference is the abundance of glycine residues. Moreover, the behavioral phenotype elicited by vi6a upon IC injection is also distinct from that of the other O1-superfamily conotoxins. As previously mentioned, intracranial (IC) injection of vi6a into mice causes hyperactivity whereas IC injection of ω-MVIIA causes shaking (Olivera et al. 1987), IC injections of κ-, δ-conotoxins cause tetanic paralysis (Shon et al. 1995; Olivera and Cruz 2001) and IC injections of μO-conotoxins causes ataxia and/or reversible coma (McIntosh et al. 1995). It appears that the family of glycine-rich conotoxins reported here is pharmacologically different from previously described O1-superfamily conotoxins. This conclusion is supported by preliminary results based on the effect of vi6a in mice upon IC injection.

Pruritogen-sensitive neurons in the mouse dorsal root ganglion (DRG)

The dorsal root ganglion (DRG) contains cell bodies of a diverse population of sensory neurons that when activated by various chemical and mechanical stimuli detect different somatosensory modes such as pain, cold, heat, and itch (Basbaum et al. 2009; Delmas et al. 2011). The different somatosensory modes detected by the DRG neurons point to the heterogeneity of the cell populations in this particular locus. It is estimated that there are >25

distinct cell populations in the DRG (Teichert et al. 2012).

Chapter 4 describes populations of cells in the DRG that respond to pruritogens (itch-causing compounds). These populations comprise a very small percentage of neurons in the DRG, however, they can still be further divided into three subpopulations. One population responds exclusively to histamine (Class A), another population responds exclusively to chloroquine (Class B), and a third and very small population respond to both histamine and chloroquine (Class C).

Our experiments revealed that the class C population (His+, CQ+) is generally homogeneous in terms of TrpV1 and bradykinin receptor (BkR) expression with TrpV1 and BkR expressed by 92 ± 4.6% 73 ± 7.4% of the cells in this population, respectively. Since this class expresses the histamine receptor, the high percent of TrpV1 expression in this population is expected since previous research has shown that TrpV1 is required for histamine-dependent itch (Shim and Oh 2007). Unexpectedly, only 14 ± 5.7% of the cells in class C population (His+, CQ+) express TrpA1 considering that all class C cells express the chloroquine receptor MrgprA3 which was reported to require TrpA1 for histamine-independent itch (Liu et al. 2009; Wilson et al. 2011). Thus, our data suggest that class C cells can signal itch through the histamine-dependent pathway. Although the possibility that class C cells can mediate histamine-independent itch cannot be ignored at this point.

The high expression of the BkR in class C cells (73 ± 7.4%) is unexpected since BkR has been traditionally associated with nociceptors and not pruriceptors. However, it was shown that application of bradykinin the ligand for

BkR into atopic dermatitis (AD) lesion causes severe itching (Hosogi et al. 2006). This result and our data suggest that class C cells mostly mediate the itching caused by bradykinin in atopic dermatitis. Moreover, these data suggest that inhibitors of BkR are potential drugs for the treatment of itch in atopic dermatitis.

Class A (His+) and class B (CQ+) are not as homogeneous as the class C cells. Only 51 ± 4.2% of class a cells express TrpV1 and 50 ± 2.4% of class B cells express TrpA1. Thus, approximately half of class A and class B cells detect itch using the Trpv1-dependent (histamine-dependent itch) and TrpA1-dependent (histamine-independent) mechanism, respectively. However, it is interesting to note that Han et al. (2012) showed that MrgprA3 expressing cells are a specific labelled line for itch. Further Wilson et al. (2011) reported that the knockout of TrpA1 did not completely abolish itch caused by chloroquine. Thus, our data indicate the possibility that the non-TrpA1 expressing cells in the class B population could also mediate itch possibly in a mechanism that does not require TrpA1. Shim et al. (2007) showed that mice lacking TrpV1 has significantly reduced itching compared to wild type mice when injected with histamine. However, knocking out TrpV1 did not completely abolish itch. Thus, the TrpV1 negative cells in class A could possibly mediate itch in a TrpV1-independent mechanism.

Future research

This research has discovered novel conotoxins that are active in mice. Further, this research also discovered different classes of neurons in the mouse

DRG that are responsive to the pruritogens histamine and chloroquine. The following research projects build on the results obtained in this thesis:

1) Identify the molecular targets of fv1a and vi6a.
2) Screen the venom of mollusk-hunting cone snails for peptides homologous to the χ-conotoxins and determine whether these peptides are pharmacologically distinct from χ-conotoxins.
3) Explore the venom of worm-hunting cone snails from other clades for the expression of O-superfamily conotoxins and identify the biological activity and pharmacology of these conotoxins.
4) Develop novel bioassays for the identification of vertebrate-active conotoxins from the venom of cone snails.
5) Determine whether TrpV1 negative and TrpA1 negative cells in classes A and B mediate itch and identify the mechanism in which these cells are activated by histamine and chloroquine.

Figure 5.1. **Sequence alignment of T-superfamily conotoxins from mollusk-hunting cone snails**. Note that the amino acids in loop 1 between Cys2 and Cys3 are highly conserved among the conotoxins whereas these amino acids are highly divergent in fv1a. A conservative substitution of leucine to methionine in c-AoIc did not affect the activity of c-AoIc against NET. (χ-MrIa accession number: GQ981407)

```
χ-AoIc      --RCCGYKMCHOC-
χ-AuId      -SVCCGYKLCFOC-
χ-MrIa      NGVCCGYKLCHOC-
fv1a        -GVCCAHTGCKOCP
                **.:. * **
```

Table 5.1. Conotoxins in the O1-superfamily.

Conotoxin	Cone snail species	Prey	Sequence	References
ω-MVIIA	*C. magus*	fish	**C**KGKGAK**C**SRLMYD**CC**TGSCRSGK**C***	Olivera et al. 1987
κ-PVIIA	*C. purpurascens*	fish	**C**RIONQK**C**FQHLDD**CC**SRK**C**NRFNK**C**V	Shon et al. 1998
δ-SVIE	*C. striatus*	fish	DG**C**SSGGTF**C**GIHOGL**CC**SEF**C**FLW**C**ITFID	Bulaj et al. 2001
μO-MrVIB	*C. marmoreus*	mollusk	A**C**SKKWEY**C**IVPILGFVY**CC**PGLI**C**GPFV**C**V	McIntosh et al. 1995

*C-terminal amidatiom; O: hydroxyproline

References

Basbaum AI, Bautista DM, Scherrer G, Julius D. 2009. Cellular and molecular mechanisms of pain. Cell 139(2): 267-284.

Bönisch H, Brüss M. 2006. The norepinephrine transporter in physiology and disease. Handb Exp Pharmacol. 175: 485-524.

Brust A, Palant E, Croker DE, Colless B, Drinkwater R, Patterson B, Schroeder C, Wilson D, Nielsen CK, Smith MT, Alewood D, Alewood PF, Lewis RJ. 2009. χ-conopeptide pharmacophore development: toward a novel class of norepinephrine transporter inhibitor (Xen2174) for pain. J Med Chem. 52(22): 6991 – 7002.

Bulaj G, Dela Cruz R, Azimi-Zonooz A, West P, Watkins M, Yoshikami D, Olivera BM. 2001. δ-conotoxin structure/function through a cladistics analysis. Biochemistry 40(44): 13201-13208.

Delmas P, Hao J, Rodat-Despoix L. 2011. Molecular mechanisms of mechanotransduction in mammalian sensory neurons. Nat Rev Neurosci. 12(3): 139-153.

Green BR, Bulaj G, Norton RS. 2014. Structure and function of μ-conotoxins, peptide based sodium channel blockers with analgesic activity. Future Med Chem. 6(15): 1677 – 1698.

Hajhashemi V, Banafshe HR, Minaiyan M, Mesdaghinia A, Abed A. 2014. Antinociceptive effects of venlafaxine in a rat model of peripheral neuropathy: role of alpha2-adrenergic receptors. Eur J Pharmacol. 738: 230-236.

Hall FS, Schwarzbaum JM, Perona MT, Templin JS, Caron MG, Lesch KP, Murphy DL, Uhl GR. 2011. A greater role for the norepinephrine transporter than the serotonin transporter in murine nociception. Neuroscience 175: 315-327.

Han L, Ma C, Liu Q, Wang HJ, Cui Y, Tang Z, Kim Y, Nie H, Qu L, Patel KN, Li Z, McNeil B, He S, Guan Y, Xiao B, LaMotte RH, Dong X. 2012. A sobpopulation of nociceptors specifically linked to itch. Nat Neurosci. 16(2): 174-182.

Hosogi M, Schmelz M, Miyachi Y, Ikoma A. 2006. Bradykinin is a potent pruritogen in atopic dermatitis: a switch from pain to itch. Pain 126(1-3): 16-23.

Liu Q, Tang Z, Surdenikova L, Kim S, Patel KN, Kim A, Ru F, Guan Y, Weng HJ, Geng Y, Undem BJ, Kollarik M, Chen ZF, Anderson DJ, Dong X. 2009. Sensory neuron-specific GPCR Mrgprs are itch receptor mediating chloroquine-induced pruritus. Cell 139(7): 1353-1365.

McIntosh JM, Hasson A, Spira ME, Gray WR, Li W, Marsh M, Hillyard DR, Olivera BM. 1995. A new family of conotoxins that block voltage-gated sodium channels. J Biol Chem. 270(28): 16796-16802.

Miljanich GP. 2004. Ziconotide: neuronal calcium channel blocker for treating severe chronic pain. Curr Med Chem. 11(23): 3029-3040.

Olivera BM, Cruz LJ. 2001. Conotoxins, in retrospect. Toxicon 39(1): 7-14.

Olivera BM, Cruz LJ, de Santos V, Le Chiminant GW, Griffin D, Zeikus R, McIntosh JM, Galyean R, Varga J, Gray WR, Rivier J. 1987. Neuronal calcium channel antagonist. Discrimination between calcium channel subtypes using ω-conotoxin from *Conus magus* venom. Biochemistry 26(8): 2086-2090.

Puillandre N, Bouchet P, Duda TF Jr, Kauferstein S, Kohn AJ, Olivera BM, Watkins M, Meyer C. 2014. Molecular phylogeny and evolution of the cone snails (Gastropoda, Conoidea). Mol Phylogenet Evol. 78: 290-303.

Shim WS, Tak MH, Lee MH, Kim M, Kim M, Koo JY, Lee CH, Kim M, Oh U. 2007. TrpV1 mediates histamine-induced itching via the activation of phospholipase A2 and 12-lipoxygenase. J Neurosci. 27(9): 2331-2337.

Shon KJ, Grilley MM, Marsh M, Yoshikami D, Hall AR, Kurz B, Gray WR, Imperial JS, Hillyard DR, Olivera BM. 1995. Purification, characterization and cloning of the lockjaw peptide from *Conus purpurascens* venom. Biochemistry 34(15): 4913-4918.

Shon KJ, Stocker M, Terlau H, Stühmer W, Jacobsen R, Walker C, Grilley M, Watkins M, Hillyard DR, Gray WR, Olivera BM. 1998. κ-Conotoxin PVIIA: a peptide inhibiting the *Shaker* K^+ channel. J Biol Chem. 273(1): 33-38.

Teichert RW, Raghuraman S, Memon T, Cox JL, Foulkes T, Rivier JE, Olivera BM. 2012. Characterization of two neuronal subclasses through constellation pharmacology. Proc Natl Acad Sci. 109(31): 12758-12763.

Wilson SR, Gerhold KA, Bifolck-Fisher A, Liu Q, Patel KN, Dong X, Bautista DM. 2011. TRPA1 is required for histamine-independent, Mas-related G protein-coupled receptor-mediated itch. Nat Neurosci. 14(5): 595-602.

Zhou J. 2004. Norepinephrine transporter inhibitors and their therapeutic potential. Drugs Future 29(12): 1235-1244.